Theory of melted flux liquids

David R. Nelson and H. Sebastian Seung
Department of Physics, Harvard University, Cambridge, Massachusetts 02138
(Received 17 November 1988; revised manuscript received 20 January 1989)

Novel intermediate flux states should be accessible in high-T_c superconductors, where it appears that the conventional Abrikosov flux lattice is melted over a significant portion of the (H,T) plane. We discuss the Lindemann criterion, and argue that fluctuations in a flux crystal are highly anisotropic, so that an asymptotically two-dimensional melting transition is possible as the shear modulus drops toward zero for many sample geometries and field orientations. We then describe the "entangled flux liquid" which arises at high-flux densities or thick samples. The statistical mechanics of this liquid is closely related to the physics of two-dimensional superfluids. The decay of vortex line correlations along the field direction is controlled by the superfluid excitation spectrum. A renormalization-group analysis shows how line wandering changes the nature of the $B(H)$ constitutive relation near H_{c1}. We suggest that a heavily entangled flux liquid could exhibit a shear modulus on experimental time scales, in analogy with viscoelastic behavior in dense polymer melts.

I. INTRODUCTION

The short intrinsic coherence lengths and large critical temperatures in the recently discovered CuO_2-based superconductors suggest that these materials may exhibit novel fluctuation effects, regardless of the underlying microscopic mechanism[1] responsible for the superconductivity. Although fluctuations are usually limited to the immediate vicinity of critical points, it was recently argued that fluctuations lead to a new entangled flux liquid *phase* in a magnetic field, due to flux line wandering as vortex filaments traverse the sample.[2] Most of this analysis was carried out in the vicinity of H_{c1}, where approximations exploiting the diluteness of the vortex lines are possible.

There are now experiments indicating that the usual Abrikosov flux lattice is in fact melted over a significant portion of the (H,T) plane: Gammel *et al.*[3] have found a striking signal suggestive of flux lattice melting in single crystals of $Bi_2Sr_2CaCu_2O_8$ at temperatures well below the onset of the Meissner effect. Low-field flux flow resistivity measurements (also on bismuth compound) by van Dover *et al.*[4] show no threshold behavior for $T=50$–80 K, indicative of vortices which flow freely without a shear modulus even in the presence of pinning. These measurements are consistent with earlier observations: Although flux quanta (decorated via the Bitter technique) were observed emerging from a sample of $YBa_2Cu_3O_7$ at $T=4.2$ K, no flux patterns could be discerned at $T=77$ K, possibly due to time-dependent flux wandering in an equilibrated flux liquid.[5]

Melted flux liquids are already familiar from discussions of two-dimensional superconducting films: Dislocation-mediated melting[6] of the flux lattice leading to both ordinary and hexatic liquid phases of essentially point vortices was explored theoretically several years ago by Fisher.[7] The novelty of high-T_c superconductors lies in the possibility of a melted liquid of entangled *line* defects in three dimensions. It was argued in Ref. 2 that the high-T_c materials are especially likely to exhibit an entangled liquid regime on the basis of an analogy with superfluidity of boson world lines in $2+1$ dimensions. A related analogy was proposed by Fisher and Lee,[8] who applied duality transformations to a lattice model of a superconductor. These theories also allow for a "disentangled flux liquid" regime, which would be the three-dimensional analog of the liquid of point vortices discussed above.

In this paper we describe these ideas in more detail, in a way which makes it clear that they are not restricted to the immediate vicinity of H_{c1}. In Sec. II we discuss fluctuations in crystalline vortex arrays. The continuum elastic theory of de Gennes and Matricon[9] is used to explore the Lindemann criterion, and to show that fluctuations in the Abrikosov phase of the new superconductors become highly anisotropic needlelike objects, extended along the direction of the magnetic field. Melting becomes two-dimensional when the correlation length in this direction becomes comparable to the corresponding sample size. An asymptotically two-dimensional melting transition is possible as the bulk shear modulus drops to zero for many sample geometries and field orientations because of this pronounced anisotropy. The Lindemann criterion shows that the bulk melting temperature drops significantly as the coupling between CuO_2 planes is decreased.

In Sec. III, we discuss a free energy which models the properties of flux liquids. A criterion for entanglement is developed, based on a random-walk picture of the transverse motions of a flux line as it meanders along the direction of the applied field. The boson analogy is described, with reference to a special toroidal geometry for which it becomes exact. High-T_c superconductors correspond to exceptionally light bosons with a value of "Planck's constant" which is an order of magnitude larger than in conventional superconductors. In the toroidal geometry, there should be a Kosterlitz-Thouless phase transition from a "superfluid" entangled flux liquid to a "normal" disentangled flux liquid with decreasing magnetic field strength above H_{c1}. The boson analogy should also describe more conventional geometries, without periodic boundary conditions, provided the samples are much thicker than an entanglement correlation length.

The next two sections contain some technical calculations. In Sec. IV, we show how interacting line liquids can be mapped onto a coherent-state functional integral which differs from a similar representation for boson superfluids[10,11] only in the boundary conditions in the imaginary time direction. This representation is used to calculate the vortex line correlation function, which can be measured with neutron scattering.[12] These experiments measure fluctuations in the local density of flux lines, defined by

$$n(\mathbf{r}_\perp,z)=\sum_{i=1}^{N}\delta[\mathbf{r}_\perp-\mathbf{r}_i(z)]\,. \tag{1.1}$$

Here $\mathbf{r}_i(z)$ (see Fig. 1) is the position of the ith vortex in the (x,y) plane as it wanders along the $\hat{\mathbf{z}}$ ($\hat{\mathbf{z}}\|\mathbf{H}$) axis. Neutron scattering measures

$$S(\mathbf{q}_\perp,q_z)=\langle|n(\mathbf{q}_\perp,q_z)|^2\rangle\,, \tag{1.2}$$

where $n(\mathbf{q}_\perp,q_z)$ is the Fourier transform of $n(\mathbf{r}_\perp,z)$. The physics, however, is more conveniently discussed in terms of the partial Fourier transform

$$\begin{aligned}S(\mathbf{q}_\perp,z)&=\int_{-\infty}^{\infty}\frac{dq_z}{2\pi}e^{-iq_zz}S(\mathbf{q}_\perp,q_z)\\&=\langle n(\mathbf{q}_\perp,z+z_0)n_\perp^*(\mathbf{q}_\perp,z_0)\rangle\,.\end{aligned} \tag{1.3}$$

As illustrated in Fig. 2(a), this correlation function reduces to the structure function of a cross section of the vortex lines when $z=0$. The correlations in any such constant z cross section should be similar to those of a two-dimensional (2D) liquid. Equation (1.3) describes more generally how the Fourier components of this 2D structure function decay along the z axis due to entanglement. Our results suggest that this decay can be approximated by

$$S(\mathbf{q}_\perp,z)\approx S(\mathbf{q}_\perp,z=0)e^{-\varepsilon(q_\perp)|z|/k_BT}\,, \tag{1.4}$$

where $\varepsilon(q_\perp)$ is the excitation spectrum of the corresponding superfluid [see Fig. 2(b)]. Although our calculations are carried out using approximations suitable for a dilute superfluid gas, both the structure factor and excitation spectrum in Fig. 2 are sketched as we would expect them to be for strongly interacting 2D superfluid. Equation (1.4) corresponds to the "single-mode" approximation for superfluid dynamics. The excitation spectrum defines via

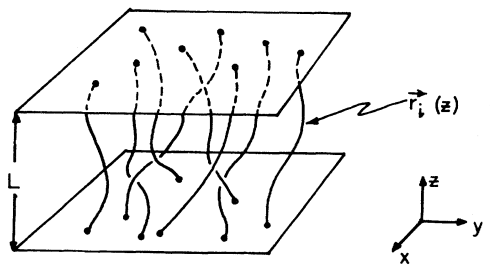

FIG. 1. Schematic of vortex lines in a slab of thickness L. The trajectory of the ith vortex along the z axis is described by the function $\mathbf{r}_i(z)$.

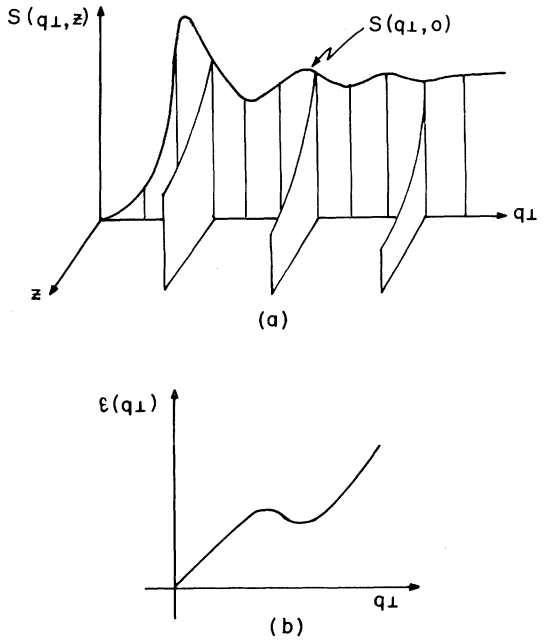

FIG. 2. (a) Partial structure function $S(\mathbf{q}_\perp,z)$ for an entangled liquid of vortex lines. For $z_\perp=0$, this quantity is just the Fourier transform of the distribution of vortices in a constant-z cross section. $S(\mathbf{q}_\perp,z)$ decays exponentially with z. (b) Boson single-particle excitation spectrum which controls the decay of the $z=0$ Fourier components (a) according to Eq. (1.4).

Eq. (1.4) a $q_\perp$-dependent correlation length

$$\xi_\parallel(q_\perp)\equiv k_BT/\varepsilon(q_\perp)\,. \tag{1.5}$$

The quantity $\xi_\parallel(q_\perp)$ is of the order of the entanglement correlation length when $q_\perp\sim 1/d$, where d is an intervortex spacing.

In Sec. V we set up a renormalization group which allows us to study the onset of flux penetration near H_{c1}. This transition is dominated by fluctuations and is a three-dimensional example of the commensurate-incommensurate transitions which have received a great deal of attention in, for example, two-dimensional rare-gas monolayers on graphite.[13] The renormalization group allows us to derive in a transparent way the fluctuation-corrected $B(H)$ constitutive relation near H_{c1},[2]

$$B(H)\approx\frac{\bar{v}}{4\pi}(H-H_{c1})\ln\left[\frac{4\pi}{\bar{v}}\frac{(\phi_0/\lambda^2)}{H-H_{c1}}\right]\,, \tag{1.6}$$

where $\phi_0=2\pi\hbar c/2e$ is the flux quantum, λ is the London penetration depth, and

$$\bar{v}=\frac{\tilde{\epsilon}_1\phi_0^2}{4\pi(k_BT)^2}\,. \tag{1.7}$$

We find that H_{c1} is renormalized downward from its mean-field value by fluctuations. Although $\tilde{\epsilon}_1$ would be the vortex line tension in an isotropic superconductor, the anisotropy of the high-T_c materials reduces this parameter by 2 orders of magnitude or more for applied fields oriented perpendicular to the CuO_2 planes. As a result,

Eq. (1.6) replaces the traditional Abrikosov result[14,15]

$$B \approx \frac{2\phi_0}{\sqrt{3}\lambda^2}\left[\ln\left(\frac{3\phi_0}{4\pi\lambda^2(H-H_{c1})}\right)\right]^{-2}, \tag{1.8}$$

over a broader range of reduced fields $[(H-H_{c1})/H_{c1} \lesssim 10^{-2}$ at $T=77$ K] than in the isotropic example worked out in Ref. 2. The weakly coupled planes and high critical temperatures of the new superconductors combine to make the dimensionless coupling constant (1.7) of order 10^4–10^5 times smaller than in conventional superconducting materials. We also discuss the behavior of the structure factor near H_{c1}.

Finally, in Sec. VI, we conclude with some speculations about the dynamics of heavily entangled liquids of flux lines. We discuss pinning, and point out that, provided barriers to line crossings are sufficiently high, regimes analogous to a heavily entangled (two-dimensional) polymer melt may be possible. In thick superconducting samples, there can be long relaxation times in the flux liquid, similar to those characterizing viscoelastic behavior in reptation theories of entangled polymers.[16] Such long relaxation times could be helpful in suppressing flux flow resistivity, because the flux liquid would exhibit a nonzero shear modulus on experimental time scales.

II. FLUX LATTICE MELTING

As discussed in the Introduction, there are strong experimental indications[3–5] that the conventional Abrikosov flux lattice of vortices is melted in high-T_c superconductors over much of the (H,T) phase diagram. The effect is particularly pronounced in Bi-Sr-Ca-Cu-O, which presumably differs from Y-Ba-Cu-O primarily in the greater effective spacing between CuO_2 planes. In Ref. 2, it was assumed for simplicity that fluctuations would melt the Abrikosov lattice in high-T_c materials whenever the intervortex spacing exceeded the range of interactions. More exact criteria, however, follow from a study of fluctuations in the crystalline phase, using the continuum elastic description of vortex line displacements proposed by de Gennes and Matricon.[9] As we shall see, the flux lattice which exists in mean-field theory[14,15] can be melted even when the vortex spacing is much less than the range of interactions. We shall restrict our attention to situations such that $H < H_{c2}(T)$, where $H_{c2}(T)$ is defined experimentally by the onset of the Meissner effect.

Although this is not essential, it will be useful to imagine for illustrative purposes that the continuum elastic theory arises from a phenomenological Ginzburg-Landau free energy in the London limit. Except near $H_{c2}(T)$, we can neglect fluctuations in the *magnitude* ψ_0 of the condensate order parameter:

$$\psi(\mathbf{r}) = \psi_0 e^{i\theta(\mathbf{r})}. \tag{2.1}$$

We assume the ψ_0 drops to zero inside a vortex core radius $\xi(T)$, which we identify with the superconducting coherence length. The Gibbs free energy for fixed external field $\mathbf{H}$ then reads[14,15,17]

$$G(\mathbf{H}) = \tfrac{1}{2}\psi_0^2\hbar^2\int d^3r\left(\partial_i\theta - \frac{2e}{\hbar c}A_i\right)M_{ij}^{-1}\left(\partial_j\theta - \frac{2e}{\hbar c}A_j\right) + \frac{1}{8\pi}\int d^3r\, b^2 - \frac{\mathbf{H}}{4\pi}\int d^3r\,\mathbf{b}, \tag{2.2}$$

where $\mathbf{b}(\mathbf{r}) = \nabla\times\mathbf{A}(\mathbf{r})$ and M_{ij} is an anisotropic effective mass tensor. For high-T_c materials, we have to an excellent approximation

$$M_{ij} = \begin{pmatrix} M_1 & 0 & 0 \\ 0 & M_1 & 0 \\ 0 & 0 & M_3 \end{pmatrix}, \tag{2.3}$$

in a coordinate system whose z axis coincides with $\hat{\mathbf{c}}$, i.e., the normal to the CuO_2 planes. M_3 is the effective mass along the z direction, while M_1 is the effective mass which describes interactions within the (x,y) plane. The equilibrium magnetic field $\mathbf{B}_0$, the spatial average of $\mathbf{b}(\mathbf{r})$, follows from minimizing (2.2) for fixed $\mathbf{H}$.

Above H_{c1}, it becomes energetically preferable for a nonzero concentration of vortex lines to enter the sample. For isotropic materials ($M_1 = M_3 \equiv M$), we can insert a triangular lattice of flux lines with areal number density

$$n \equiv B/\phi_0 \tag{2.4}$$

into Eq. (2.2), and find the approximate Gibbs energy density g per unit volume in the region $H_{c1} \ll H \ll H_{c2}$,[14,15,17]

$$g(B) \approx \frac{B^2}{8\pi} + \frac{\phi_0}{32\pi^2\lambda^2}B\ln(\alpha H_{c2}/B) - \frac{\mathbf{H}\cdot\mathbf{B}}{4\pi}. \tag{2.5}$$

Here, α is a constant of order unity, $\phi_0 = 2\pi\hbar c/2e = 2\times10^{-7}$ G cm^2, and

$$\lambda^2 = \frac{Mc^2}{4\pi\psi_0^2 e^2} \tag{2.6}$$

is the London penetration depth. The minimum value of $\mathbf{B} \equiv \mathbf{B}_0$ is parallel to $\mathbf{H}$, and is given [neglecting the weak B dependence in the logarithm in (2.5)] by the solution of

$$H = B_0 + \frac{\phi_0}{8\pi^2\lambda^2}\ln(\alpha H_{c2}/B_0). \tag{2.7}$$

The coherence length $\xi(T)$ enters only in providing a short-distance cutoff for the free energy (2.2). The ratio $\kappa = \lambda/\xi$ is extremely large in the high-T_c materials, of order $\kappa \approx 10^2$–10^3.[18] For an anisotropic superconductor with $\mathbf{B}\|\mathbf{H}\|\hat{\mathbf{z}}$, Eq. (2.5) also holds, provided we replace M by M_1 in Eq. (2.6). Although a complete treatment for general field orientations is difficult, approximate formulas have been derived by Campbell, Doria, and Kogan.[19]

In the remainder of this section, we show how thermal fluctuations decorrelate the rigid "line lattice" of vortices discussed above. The effects of these fluctuations are particularly pronounced because of the small elastic constants and high critical temperatures which characterize high-T_c materials.

A. Continuum elastic theory and the Lindemann criterion

We assume that the external field is aligned with the z direction, and describe the trajectory of the ith vortex by a function $\mathbf{r}_i(z)$. If the average position of the ith vortex in the triangular lattice discussed above is denoted by $\mathbf{R}_i$, we can define a two-dimensional displacement field $\mathbf{u}(\mathbf{R}_i,z)$ by

$$\mathbf{r}_i(z)=\mathbf{R}_i+\mathbf{u}(\mathbf{R}_i,z)\,. \tag{2.8}$$

In the continuum limit, this displacement becomes a function $\mathbf{u}=\mathbf{u}(x,y,z)$. The excess free energy $\delta G[\mathbf{u}(\mathbf{r})]$ associated with small gradients of $\mathbf{u}$ is[9]

$$\delta G[\mathbf{u}(\mathbf{r})]=\frac{1}{2}\int d^3r\left[2\mu u_{\alpha\beta}^2+\lambda u_{\delta\delta}^2+K\left(\frac{\partial\mathbf{u}}{\partial z}\right)^2\right], \tag{2.9}$$

where

$$u_{\alpha\beta}(\mathbf{r})=\frac{1}{2}\left(\frac{\partial u_\alpha}{\partial r_\beta}+\frac{\partial u_\beta}{\partial r_\alpha}\right),\quad \alpha,\beta=x,y \tag{2.10}$$

is the symmetrized two-dimensional strain matrix, μ and λ are Lamé coefficients, and K is a tilt elastic constant. We use the same symbol for the Lamé coefficient λ as for the London penetration depth. Which quantity we mean should be clear from the context.

As pointed out by de Gennes and Matricon, two constraints on these three elastic constants are provided by the macroscopic magnetic properties of the material. For a uniform dilation of the area A perpendicular to the z axis we have

$$\partial_x u_x+\partial_y u_y=\delta A/A\,, \tag{2.11}$$

where δA is the change in area. The increase in energy according to (2.9) is $\delta G\equiv V\delta g$, with

$$\begin{aligned}\delta g&=\tfrac{1}{2}(\mu+\lambda)(\delta A/A)^2\\&=\tfrac{1}{2}(\mu+\lambda)(\delta B/B)^2\,,\end{aligned} \tag{2.12}$$

and where V is the volume. The last line follows because $BA=N\phi_0=$const during the dilation. We can, on the other hand, also calculate this increased energy directly by expanding Eq. (2.5) about the minimum at $\mathbf{B}=\mathbf{B}_0$. Upon setting $\mathbf{B}=\mathbf{B}_0+\delta\mathbf{B}_\parallel+\delta\mathbf{B}_\perp$, where $\delta\mathbf{B}_\parallel$ and $\delta\mathbf{B}_\perp$ are small deviations parallel and perpendicular to $\mathbf{B}_0\|\mathbf{H}$, we find (again neglecting the B dependence of the logarithm)

$$\begin{aligned}\delta g(\mathbf{B})&=g(\mathbf{B})-g(\mathbf{B}_0)\\&=\frac{1}{8\pi}|\delta\mathbf{B}_\parallel|^2+\frac{1}{8\pi}\left(\frac{H}{B_0}\right)|\delta\mathbf{B}_\perp|^2.\end{aligned} \tag{2.13}$$

For the small dilation discussed above, $\delta\mathbf{B}_\perp=0$, so comparison of (2.13) with (2.12) shows that the bulk modulus of the line lattice is

$$\mu+\lambda\approx\frac{B_0^2}{4\pi}\,. \tag{2.14}$$

More generally, the sum $\mu+\lambda$ is given by $\mu+\lambda=B_0^2/4\pi\mu_z$, where $\mu_z=dB(H)/dH$ is the longitudinal magnetic permeability.[9]

Imposing a uniform tilt on the vortex lines leads to a second constraint on the elastic constants. If the vortex lines are all inclined at a small angle θ to the z axis, a small transverse magnetic field $|\delta\mathbf{B}_\perp|\approx B_0\theta$ is generated, and the increased energy per unit volume from Eq. (2.9) is

$$\begin{aligned}\delta g&=\tfrac{1}{2}K\theta^2\\&=\tfrac{1}{2}K|\delta\mathbf{B}_\perp|^2/B_0^2\,.\end{aligned} \tag{2.15}$$

Comparison with Eq. (2.13) shows that the tilt modulus is[9]

$$K=\frac{HB_0}{4\pi}\,. \tag{2.16}$$

Henceforth, we will drop the subscript 0 on the equilibrium magnetic field, and set $B_0\equiv B$. The relation (2.16) is in fact exact for any rotationally invariant superconductor. The tilt modulus will be much smaller, however, for anisotropic high-T_c superconductors with weakly coupled planes. For $\mathbf{H}\|\hat{\mathbf{z}}$, a reasonable guess (which becomes exact for low fields) might be

$$K\approx\frac{M_1}{M_3}\frac{HB}{4\pi}\,. \tag{2.17}$$

Note that K vanishes as M_3^{-1} for large M_3, as is physically reasonable when the coupling between planes tends to zero. If, following Campbell, Doria, and Kogan,[19] the ratio M_1/M_3 is estimated from the upper critical fields parallel and perpendicular to the z axis $[M_1/M_3=(H_{c2}^{\parallel}/H_{c2}^{\perp})^2]$,[18] one finds $M_1/M_3\approx10^{-2}$. The tilt modulus is clearly bounded above by the isotropic result (2.16). For $H\gg H_{c1}$, we can set $B=H$ in (2.17).

The only elastic constant not determined directly by the magnetic properties is the shear modulus. The shear modulus is typically much smaller than the bulk modulus for all regimes of interest, and actually vanishes near H_{c2}, as shown by Labusch[20]

$$\mu\approx7\times10^{-3}\left(\frac{H_{c2}}{\kappa}\right)^2(1-H/H_{c2})^2\,. \tag{2.18}$$

We shall use (2.18) to approximate μ for $\frac{1}{2}H_{c2}\lesssim H\leq H_{c2}$. For the opposite limit of $H_{c1}\leq H\lesssim\frac{1}{2}H_{c2}$, we can use the result of Fetter, Hohenberg, and Pincus:[21]

$$\mu\approx\tfrac{1}{4}B\phi_0/(4\pi\lambda)^2\,. \tag{2.19}$$

These are zero-temperature results for shear distortions of triangular Abrikosov lattices with flux lines regarded as rigid rods. At finite temperatures, the shear modulus will be renormalized downward by fluctuations, as already calculated for the case of two-dimensional point vortices by Fisher.[7] In three dimensions, the random-walk-like vortex fluctuations discussed elsewhere in this paper will produce a similar softening of both the shear and the tilt moduli.

We are now in a position to estimate the mean-square

displacement of a flux line,[22,23] i.e.,

$$\langle|\mathbf{u}(\mathbf{r}_0)|^2\rangle=\frac{\int\mathcal{D}\mathbf{u}(\mathbf{r})\,|\mathbf{u}(\mathbf{r}_0)|^2 e^{-\delta G/k_BT}}{\int\mathcal{D}\mathbf{u}(\mathbf{r})e^{-\delta G/k_BT}}$$
$$=\int\frac{d^3q}{(2\pi)^3}\left(\frac{k_BT}{\mu q_\perp^2+Kq_z^2}+\frac{k_BT}{(2\mu+\lambda)q_\perp^2+Kq_z^2}\right) \tag{2.20}$$

where $q_\perp^2=q_x^2+q_y^2$. We take the cutoff to infinity in the z direction, and impose for simplicity a circular cutoff Λ in the (x,y) plane. We choose $\Lambda=\sqrt{4\pi n}$ which conserves the area of the hexagonal Brillouin zone. The mean-square displacement is then

$$\langle|\mathbf{u}(\mathbf{r}_0)|^2\rangle=\left(\frac{n}{4\pi}\right)^{1/2}\left(\frac{k_BT}{(\mu K)^{1/2}}+\frac{k_BT}{[(2\mu+\lambda)K]^{1/2}}\right). \tag{2.21}$$

Because the shear modulus tends to zero at H_{c2}, $\langle|\mathbf{u}(\mathbf{r})|^2\rangle$ diverges in this approximation, suggesting that the Abrikosov flux lattice may melt, as originally pointed out by Labusch.[20] The shear modulus is small relative to the bulk modulus at all fields, so we can always neglect the second term in Eq. (2.21). Upon inserting the estimates (2.18) and (2.17) for μ and K appropriate for $H\gtrsim\frac{1}{2}H_{c2}$, we find

$$\langle|\mathbf{u}(\mathbf{r})|^2\rangle\approx\left(\frac{n}{4\pi K\mu}\right)^{1/2}k_BT$$
$$\approx(12\kappa k_BT)\left(\frac{M_3}{M_1\phi_0^3H_{c2}}\right)^{1/2}\frac{h^{1/2}}{1-h}d^2, \tag{2.22}$$

where $d\approx\sqrt{\phi_0/B}$ is the spacing between vortex lines, and the reduced field $h=H/H_{c2}$.

Taking as parameters for Ba-Sr-Ca-Cu-O $\kappa=2\times10^2$, $H_{c2}(T=77\text{ K})=2\times10^4$ Oe, and $(M_3/M_1)^{1/2}=15$, we find that the root-mean-square fluctuation in the line displacement at liquid-nitrogen temperatures is

$$\sqrt{\langle|\mathbf{u}|^2\rangle}\approx0.2\frac{h^{1/4}}{(1-h)^{1/2}}d. \tag{2.23}$$

Since most solids melt when the rms displacement becomes of order $\frac{1}{10}$ of the interparticle spacing, the flux lattice in the Ba-Sr-Ca-Cu-O compounds should indeed be melted for a wide range of fields,[3] at least for $\mathbf{H}\|\hat{\mathbf{z}}$. A number of comments seem appropriate at this point.

(1) For fields applied *perpendicular* to the z axis, the tilt modulus will be anisotropic and much larger than suggested by Eq. (2.17). Kogan and Campbell have suggested, however, that the modulus for shears parallel to the CuO_2 planes is very low in this case.[24] It is possible that these two effects combine to produce fluctuations of the same order as for $\mathbf{H}\|\hat{\mathbf{z}}$, as seems to be the case experimentally for Ba-Sr-Ca-Cu-O.[3] The generalization of the de Gennes–Matricon elastic free energy (2.9) is complicated, however, when vortex lines run parallel to the weakly coupled CuO_2 planes. This system is not even approximately invariant under rotations about $\mathbf{H}$: The *antisymmetric* counterpart of the strain matrix (2.10) will enter in an important way.[25]

(2) If we take as parameters for Y-Ba-Cu-O $\kappa=10^2$, $H_{c2}(T=77\text{ K})=5\times10^4$ Oe, and $(M_3/M_1)^{1/2}=5$, Eq. (2.23) is replaced by

$$\sqrt{\langle|\mathbf{u}|^2\rangle}\approx0.06\frac{h^{1/4}}{(1-h)^{1/2}}d, \tag{2.24}$$

showing that it is necessary to take H closer to H_{c2} than in Ba-Sr-Ca-Cu-O to obtain large vortex line fluctuations, as is observed experimentally.[3] These fluctuations are negligible in conventional superconductors except for fields inaccessibly close to H_{c2}.

(3) We can also evaluate Eq. (2.21) in the small-field limit $H\ll H_{c2}$ using the weak-field formula (2.19) for the shear modulus. The lattice is again essentially incompressible, and we have using Eq. (2.17) for K,

$$\langle|\mathbf{u}|^2\rangle\approx\left(\frac{n}{4\pi\mu K}\right)^{1/2}$$
$$\approx\frac{8\pi\lambda k_BT}{\phi_0^2}\left(\frac{M_3}{M_1}\right)^{1/2}\left(\frac{B}{H}\right)^{1/2}d^2. \tag{2.25}$$

Upon setting $\lambda=6000$ Å and using the parameters quoted above for Ba-Sr-Ca-Cu-O we find $\langle|\mathbf{u}|^2\rangle^{1/2}=0.08(B/H)^{1/2}d$, suggesting that, although fluctuations may be (barely) sufficient to melt the crystal when, say, $B=0.8H$, the crystal will become stable as B drops to zero near H_{c1}. This, however, is precisely the region where flux line wandering, neglected in the mean-field calculation of the shear modulus,[21] becomes most important.[2] As we show in Sec. V, interactions between vortex lines are renormalized to zero by these fluctuations as $H\to H_{c1}$. We expect that the same fluctuations will diminish the shear modulus and melt the solid in the limit $H\to H_{c1}$ at all nonzero temperatures. The same conclusion was reached in Ref. 2 on the basis of an analogy with two dimensional bosons.

(4) The Lindemann condition discussed above is a *criterion,* and not a *theory* of melting. It does not attempt to explain the melting mechanism in detail, nor does it provide an explanation of the apparently continuous changes during melting observed by Gammel *et al.*[3] The Lindemann criterion assumes wave-vector-independent elastic constants which can be a gross oversimplification, especially if fluctuations are important. The integral in (2.20) is in fact dominated by $q\sim1/d$. A more accurate theory would use wave-vector-dependent elastic constants under the integral sign in Eq. (2.20).

In the next subsection, we discuss the size and shape of the fluctuations which lead to the increase in $\langle u^2\rangle$. These are anisotropic needles, whose size and aspect ratio diverge as the shear modulus tends to zero. This pronounced anisotropy suggests that melting can in fact be asymptotically two dimensional for a variety of sample geometries and field orientations.

B. Anisotropic correlation lengths and two-dimensional melting

Most experiments on single crystals of high-T_c materials have been carried out in a slab geometry, with the short dimension along the z axis, normal to the CuO_2 planes. The mean-field theory of the bulk material predicts a second-order phase transition at H_{c2}, where, according to Eq. (2.18), the shear modulus goes continuously to zero. In Ba-Sr-Ca-Cu-O, the actual melting transition occurs well below the mean field $H_{c2}(T)$.[3] We shall assume that the renormalized shear modulus becomes very small at this (apparently continuous) transition, just as it does near H_{c2} in mean-field theory. Associated with the drop in the shear modulus is a diverging correlation volume for fluctuations which decorrelate the crystalline order. When the size of this correlation volume becomes comparable to the appropriate sample dimension (e.g., the slab thickness, for $\mathbf{H}\|\hat{\mathbf{z}}$), the system crosses over from three- to two-dimensional behavior. Such a crossover to two-dimensional melting of the flux lattice for $\mathbf{H}\|\hat{\mathbf{z}}$ has been proposed by Markiewicz[26] and by Gammel *et al.*[3] Although the crossover will not greatly affect the melting temperature in most samples, it will determine the asymptotic critical behavior at the transition itself. Here, we calculate the dimensions of the bulk correlation volume, and show that it is characterized by *two* diverging correlation lengths, one parallel to the field direction and one perpendicular to it. These fluctuations are anisotropic needle-shaped objects, and can lead to two-dimensional melting close to the transition for many sample geometries and field orientations.

The correlation lengths in question can be measured directly using neutron scattering,[12] which probes correlations in the vortex line density defined by Eq. (1.1). The behavior of the structure function (1.2) near a (two-dimensional) reciprocal-lattice vector $\mathbf{G}$ of the flux lattice is given by the Fourier transform of[6]

$$C_{\mathbf{G}}(\mathbf{r}_\perp,z)=\langle\exp\{i\mathbf{G}\cdot[\mathbf{u}(\mathbf{r}_\perp,z)-\mathbf{u}(\mathbf{0},0)]\}\rangle . \tag{2.26}$$

For fields parallel to $\hat{\mathbf{z}}$, this correlation function is easily evaluated using the de Gennes–Matricon free energy (2.9),

$$\begin{aligned}C_{\mathbf{G}}(\mathbf{r}_\perp,z)&=\exp\{-\tfrac{1}{2}G_iG_j\langle[u_i(\mathbf{r}_\perp,z)-u_i(\mathbf{0},0)][u_j(\mathbf{r}_\perp,z)-u_j(\mathbf{0},0)]\rangle\}\\&=\exp\left[-G_iG_j\int\frac{d^3q}{(2\pi)^3}(1-e^{i\mathbf{q}\cdot\mathbf{r}})\left(\frac{k_BT}{\mu q_\perp^2+Kq_z^2}P_{ij}^T(\mathbf{q}_\perp)+\frac{k_BT}{(2\mu+\lambda)q_\perp^2+Kq_z^2}P_{ij}^L(\mathbf{q}_\perp)\right)\right],\end{aligned} \tag{2.27}$$

where $\mathbf{r}\equiv(\mathbf{r}_\perp,z)$ and $P_{ij}^T(\mathbf{q}_\perp)$ and $P_{ij}^L(\mathbf{q}_\perp)$ are two-dimensional transverse and longitudinal projection operators. For large separations, $C(\mathbf{r}_\perp,z)$ tends to $\exp(-\frac{1}{2}G^2\langle u^2\rangle)$, i.e., to the Debye-Waller factor associated with the reciprocal-lattice vector $\mathbf{G}$. For points separated primarily along the z direction, there is a $1/z$ approach to this constant,

$$C_{\mathbf{G}}(\mathbf{r}_\perp,z)\underset{z\to\infty}{\approx}\exp(-\tfrac{1}{2}G^2\langle u^2\rangle)\times\left[1+\frac{k_BTG^2}{8\pi}\left(\frac{1}{\mu}+\frac{1}{2\mu+\lambda}\right)\frac{1}{z}\right]. \tag{2.28}$$

To define a correlation length, we consider the smallest nonzero reciprocal-lattice vector, with magnitude $|\mathbf{G}|=G_0=4\pi/\sqrt{3d}$ for a triangular lattice. Following a similar analysis for superfluid helium by Hohenberg *et al.*,[27] we extract a longitudinal correlation length ξ_z by setting

$$C_{\mathbf{G}}\equiv\exp(-\tfrac{1}{2}G^2\langle u^2\rangle)(1+\xi_z/z)$$

for large z and find

$$\xi_z=\frac{k_BTG_0^2}{8\pi}\left(\frac{1}{\mu}+\frac{1}{2\mu+\lambda}\right)\approx\frac{k_BTG_0^2}{8\pi\mu}. \tag{2.29}$$

As shown schematically in Fig. 3, ξ_z is the scale over which the translational order parameter $\Psi_{\mathbf{G}}(\mathbf{r}_\perp,z)=\exp[i\mathbf{G}\cdot\mathbf{u}(\mathbf{r}_\perp,z)]$ of the Abrikosov flux lattice relaxes to its equilibrium value along $\hat{\mathbf{z}}$. For separations which are primarily perpendicular to $\hat{z}$, we find

$$C_{\mathbf{G}}(\mathbf{r}_\perp,z)\underset{r_\perp\to\infty}{\approx}\exp(-\tfrac{1}{2}G^2\langle u^2\rangle)\left[1+\frac{k_BTG^2}{8\pi}\left(\frac{1}{(\mu K)^{1/2}}+\frac{1}{[(2\mu+\lambda)K]^{1/2}}\right)\frac{1}{r_\perp}\right]. \tag{2.30}$$

The corresponding perpendicular correlation length perpendicular to $\hat{\mathbf{z}}$ is

$$\xi_\perp=\frac{k_BTG_0^2}{8\pi}\left(\frac{1}{(\mu K)^{1/2}}+\frac{1}{[(2\mu+\lambda)K]^{1/2}}\right)\approx\frac{k_BTG_0^2}{8\pi(\mu K)^{1/2}}. \tag{2.31}$$

The quantities ξ_z and $\xi_\perp$ are *translational* correlation lengths, and should not be confused with the superconducting coherence length.

Upon using the approximations (2.17) and (2.18) for K and μ and the material parameters for Ba-Sr-Ca-Cu-O, we find (with $T=30$ K)

$$\xi_z\approx(300k_BT\kappa^2/\Phi_0H_{c2})\frac{h}{(1-h)^2}\approx(5.2\times10^{-6}\text{ cm})\frac{h}{(1-h)^2} \tag{2.32a}$$

and

$$\xi_\perp=(90k_BT\kappa/\Phi_0H_{c2})\left(\frac{M_3}{M_1}\right)^{1/2}\frac{1}{(1-h)}\approx(1.1\times10^{-7}\text{ cm})\frac{1}{(1-h)}. \tag{2.32b}$$

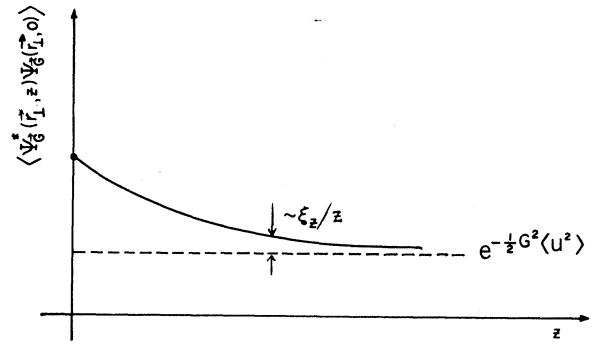

FIG. 3. Translational correlation function for the Abrikosov flux lattice. This correlation function tends to a nonzero constant for large z, given by the Debye-Waller factor of the crystal. There is a $1/z$ approach to this constant, which allows us to define a translational correlation length in the z direction, ξ_z. This length determines the size of fluctuations along the field direction. The analogous correlation length perpendicular to z is much shorter, $\xi_\perp \ll \xi_z$.

Note that both the aspect ratio and the dimensions of the coherence region (which has volume $\xi_z\xi_\perp^2$) diverge as $H \to H_{c2}$. Provided these divergences are not preempted by a bulk first-order phase transition, the melting transition will eventually become two-dimensional when ξ_z becomes comparable to the sample dimension along $\hat{\mathbf{z}}$. Although this only happens close to H_{c2} in mean-field theory, the crossover to two-dimensional melting will occur at a lower temperature if fluctuations renormalize μ toward zero at this point. The large mean-field value of ξ_z in Eq. (2.32a) makes it plausible that this correlation length could become comparable to the 0.01-cm slab thickness in the experiments of Ref. 3 when $\mathbf{H}\|\hat{\mathbf{z}}$, especially when the softening of shear modulus due to three-dimensional fluctuations is taken into account.

The aspect ratio of the correlation volume is

$$\frac{\xi_z}{\xi_\perp}=\left[\frac{K}{\mu}\right]^{1/2}=3.3\kappa\left[\frac{M_1}{M_3}\right]^{1/2}\frac{h}{(1-h)}, \tag{2.33}$$

which is especially large for Ba-Sr-Ca-Cu-O. If this aspect ratio has the same large value for $\mathbf{H}\perp\hat{\mathbf{z}}$, it will be more than five times larger than the aspect ratio of the *sample* studied by Gammel *et al.*[3] Thus, correlations along the flux lines will reach the 0.1-cm slab width when perpendicular correlation length is only a fraction of the 0.01-cm slab thickness. Continuous two-dimensional melting may be possible both for $\mathbf{H}\|\hat{\mathbf{z}}$ and $\mathbf{H}\perp\hat{\mathbf{z}}$, consistent with experiments of Ref. 3. Melting of the anisotropic flux lattice for $\mathbf{H}\perp\hat{\mathbf{z}}$ would presumably proceed according to the two-dimensional anisotropic melting theory of Ostlund and Halperin.[28]

The correlation lengths (2.29) and (2.31) depend on the renormalized shear modulus at long wavelengths. More work is needed on the bulk fluctuations which actually cause the shear modulus to become small well below the mean field H_{c2}. If the anisotropy of these fluctuations really does lead to continuous two-dimensional melting, a (possibly small) region of *hexatic* line liquid will exist just above the transition.[6] In the remainder of this paper we investigate only flux liquids which are *isotropic* in the plane perpendicular to $\mathbf{H}$.

We note finally that it is easy to Fourier transform (2.27) and thus obtain the behavior of the structure function near a reciprocal-lattice vector. The result is a δ-function Bragg peak at $\mathbf{G}$ with strength $\exp(-\frac{1}{2}G^2\langle u^2\rangle)$, as well as a thermal diffuse background whose strength depends on the elastic constants. Upon setting $\mathbf{q}=\mathbf{G}+\mathbf{k}$, we find that, for $k \ll G_0$,

$$S(\mathbf{q},q_z)\approx\exp(-\tfrac{1}{2}G^2\langle|\mathbf{u}|^2\rangle)\left[\delta(\mathbf{k})+G_iG_j\frac{k_BT}{\mu k_\perp^2+Kk_z^2}P_{ij}^T(\mathbf{k}_\perp)+G_iG_j\frac{k_BT}{(2\mu+\lambda)k_\perp^2+Kk_z^2}P_{ij}^L(\mathbf{k}_\perp)\right]. \tag{2.34}$$

Upon neglecting the last term, we see that the contours of constant diffuse scattering for $\mathbf{k}_\perp\perp\mathbf{G}$ are ellipses centered on $\mathbf{G}$, with short axis along $\hat{\mathbf{z}}$. These squashed diffuse scattering contours reflect the needlelike shape of the fluctuations in real space.

III. FREE ENERGY OF LINE LIQUIDS AND BOSON ANALOGY

In this section, we describe a model free energy for the statistical mechanics of flux liquids. A qualitative picture of the entangled flux liquid follows from an analogy with boson superfluidity in two dimensions. This analogy becomes exact in a toroidal geometry which would be especially interesting to explore experimentally. Some of the results of this section were summarized in Ref. 2.

A. Model free energy and flux line wandering

We work in the London limit, and describe the ith vortex line in a sample of thickness L by the function $\mathbf{r}_i(z)=[x_i(z),y_i(z)]$, as illustrated in Fig. 1. The Gibbs free energy of N interacting flux lines in an *isotropic* superconductor with applied field $\mathbf{H}$ reads[14,15]

$$G(\mathbf{H})=\sum_{i=1}^{N}\epsilon_1\int_0^L dz\left[1+\left|\frac{d\mathbf{r}_i}{dz}\right|^2\right]^{1/2}+\tfrac{1}{2}\sum_{i\neq j}\int_0^L dz\,V[\mathbf{r}_i(z)-\mathbf{r}_j(z)]-\frac{\mathbf{H}}{4\pi}\int d^3r\,\mathbf{b}(\mathbf{r}), \tag{3.1}$$

where the line tension ϵ_1 is given in terms of the London penetration depth λ by $\epsilon_1=(\phi_0/4\pi\lambda)^2\ln\kappa$. The interaction potential $V(\mathbf{r})$ between pairs of vortex lines is

$$V(\mathbf{r})=\frac{\phi_0^2}{8\pi^2\lambda^2}K_0(|\mathbf{r}|/\lambda), \tag{3.2}$$

where $K_0(x)$ is the modified Bessel function, $K_0(x)\approx(\pi/2x)^{1/2}e^{-x}$ for large x. We have assumed that the vortex coordinates vary slowly with z, so that we can use a

potential which is local in z: a vortex at height z interacts only with other vortices in the same constant z cross section, an approximation which is only strictly valid when all vortices are parallel to z.

Upon expanding the square root in the line energy and reexpressing the integral of $\mathbf{b}(r)$ in terms of the flux quantum and the number of vortices we have

$$G(\mathbf{H}) = \left(\epsilon_1 - \frac{H\phi_0}{4\pi}\right) NL + \tfrac{1}{2}\tilde{\epsilon}_1 \sum_{i=1}^{N} \int_0^L dz \left|\frac{d\mathbf{r}_i}{dz}\right|^2 + \tfrac{1}{2}\sum_{i\neq j}\int_0^L dz\, V[\mathbf{r}_i(z)-\mathbf{r}_j(z)]\,, \tag{3.3}$$

where the coefficient of the second term $\tilde{\epsilon}_1$ equals ϵ_1 in the isotropic case. To treat *anisotropic* superconductors with $\mathbf{H}$ perpendicular to the CuO_2 planes, we note first that $|d\mathbf{r}_i(z)/dz|^2 \approx \theta_i^2(z)$, where $\theta_i(z)$ is the local angle of inclination on the ith vortex line to the z axis. The line tension is a function of this angle when the effective-mass tensor is anisotropic as in Eq. (2.3),[17]

$$\epsilon_1(\theta) = \left(\frac{\phi_0}{4\pi\lambda}\right)^2 \ln\kappa \left(\frac{M_1}{M_3}\sin^2\theta + \cos^2\theta\right)^{1/2} \approx \epsilon_1\left(1+\frac{1}{2}\frac{M_1-M_3}{M_3}\theta^2\right), \tag{3.4}$$

where we have expanded in θ and set $\epsilon_1 = (\phi_0/4\pi\lambda)^2 \ln\kappa$ to obtain the second line. Here, λ is given by Eq. (2.6), with M replaced by M_1. The total line energy E_i of the ith line is thus

$$E_i = \int_0^L dz\, \epsilon_1(\theta_i)\left(1+\left|\frac{d\mathbf{r}_i}{dz}\right|^2\right)^{1/2} \approx \epsilon_1 L + \tfrac{1}{2}\epsilon_1\frac{M_1}{M_3}\int_0^L dz\left(\frac{d\mathbf{r}_i}{dz}\right)^2. \tag{3.5}$$

The free energy for anisotropic superconductors then has the form (3.3), with

$$\tilde{\epsilon}_1 = \frac{M_1}{M_3}\epsilon_1\,. \tag{3.6}$$

A full statistical treatment of the partition function associated with Eq. (3.3) entails integration of $\exp(-G/k_BT)$ over all vortex trajectories $\{r_i(z)\}$. The partition function, for example, is

$$Z = \sum_{N=0}^{\infty}\frac{1}{N!}\int \mathcal{D}\mathbf{r}_1(z)\cdots\int \mathcal{D}\mathbf{r}_N(z)\, e^{-G/k_BT}. \tag{3.7}$$

The vortex lines are like the world lines of particles, where the z coordinate plays the role of time. This problem is usually treated in the mean-field approximation, assuming rigid vortex lines and neglecting the "kinetic energy" contribution proportional to $|d\mathbf{r}_i(z)/dz|^2$ in Eq. (3.3).[14,15] At $T=0$ vortices first penetrate the sample when the "chemical potential" term in (3.3) changes sign, i.e., for $H > H_{c1}$, where

$$H_{c1} = 4\pi\epsilon_1/\phi_0\,. \tag{3.8}$$

Minimizing with respect to the areal density $n = B/\phi_0$ of a triangular lattice of flux lines then leads to the standard Abrikosov result (1.8) for the $B(H)$ constitutive relation.

This treatment of the onset of flux line penetration is similar to the Frank–van der Meer theory of misfit dislocations near the commensurate-incommensurate transition in, e.g., krypton absorbed on graphite. This zero-temperature theory becomes incorrect at finite temperature due to dislocation line wandering.[13] The usual Abrikosov theory leading to Eq. (1.8) breaks down in a similar way at the elevated temperatures of the high-T_c superconductors: the "kinetic energy" dominates the potential energy in Eq. (3.3). Although a complete theory of the statistical mechanics near H_{c1} will be worked out in Sec. V, we can estimate when the Abrikosov theory breaks down from a simple random-walk argument.[2] We consider a single flux line $\mathbf{r}(z)$ and determine how far it wanders perpendicular to the z axis as it traverses the sample. The relevant path integral is

$$\langle|\mathbf{r}(z)-\mathbf{r}(0)|^2\rangle = \frac{\int \mathcal{D}\mathbf{r}(s)\,|\mathbf{r}(z)-\mathbf{r}(0)|^2 \exp\left[-(\tilde{\epsilon}_1/2k_BT)\int_0^L (d\mathbf{r}/ds)^2 ds\right]}{\int \mathcal{D}\mathbf{r}(s)\exp\left[-(\tilde{\epsilon}_1/2k_BT)\int_0^L (d\mathbf{r}/ds)^2 ds\right]} = \frac{2k_BT}{\tilde{\epsilon}_1}|z|\,, \tag{3.9}$$

which shows that the vortex "diffuses" as a function of the timelike variable z,

$$\sqrt{\langle|\mathbf{r}(z)-\mathbf{r}(0)|^2\rangle} = \sqrt{2D|z|}\,, \tag{3.10}$$

with diffusion constant

$$D = k_BT/\tilde{\epsilon}_1 = \frac{M_3}{M_1}\frac{4\pi k_BT}{\phi_0 H_{c1}}\,. \tag{3.11}$$

At $T=77$ K, we take $H_{c1}\approx 10^2$ G and $M_3/M_1 \approx 10^2$ and find $D = 10^{-6}$ cm, so that vortex lines wander a distance of order 1 μm while traversing a sample of thickness 0.01 cm.

Following the treatment of commensurate-incommensurate transitions in Ref. 13, we note that collisions between neighboring vortices will reduce the configurational entropy in the partition function (3.7). As shown in Ref. 2, this effect dominates the weak repulsive interaction in Eq. (3.2) close to H_{c1} in sufficiently thick samples. More generally, we can define an entanglement correlation length

$$\xi_z \equiv \frac{1}{2Dn} = \frac{\tilde{\epsilon}_1}{2k_BTn}\,, \tag{3.12}$$

which is the spacing between collisions in a vortex liquid with areal density $n = B/\phi_0$. Collisions and entanglement of vortex lines will significantly alter the Abrikosov theory whenever

$$L \gg \xi_z\,. \tag{3.13}$$

B. Analogy with boson statistical mechanics in two dimensions

It is not hard to show that the transfer matrix connecting neighboring constant-z slices of the partition function (3.7) is just the exponential of the N-particle Hamiltonian operator in imaginary time for quantum-mechanical particles interacting with the potential (3.2) (see Sec. IV). Indeed, Eq. (3.7) is just the imaginary time Feynman path integral[29] for this problem with free boundary conditions for the particle world lines. The statistical mechanics as $L \rightarrow \infty$ will be dominated by the ground-state wave function. Although there is no *a priori* requirement that the solutions of this Schrödinger equation obey boson or fermion statistics, one can show quite generally that the *ground-state* wave function is bosonic.[29]

To extend this analogy to finite L, it is helpful to first consider the special experimental geometry with a toroidal magnetic field shown in Fig. 4. The vortex trajectories $\{\mathbf{r}_i(s)\}$ are now functions of arc length s around the torus instead of z. The partition function differs from Eq. (3.7) in that we must now impose periodic boundary conditions

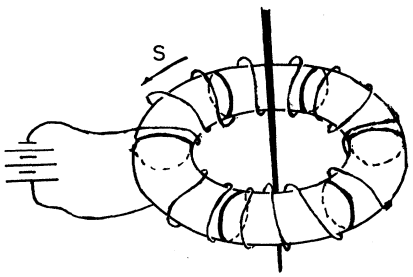

FIG. 4. Toroidal superconducting sample in a toroidal magnetic field for which the analogy with the statistical mechanics of two-dimensional bosons becomes exact.

on the vortex lines: A configuration of vortices in any given circular cross section must return to itself when the vortex lines are followed around the torus. To completely sample the allowed phase space, we must sum over different ways of connecting the vortices as they traverse the circuit. The partition function (3.7) is replaced by

$$Z' = \sum_{N=0}^{\infty} \frac{1}{N!} \sum_{P} \int_{\mathbf{r}_1(L)=P[\mathbf{r}_1(0)]} \mathcal{D}\mathbf{r}_1(s) \cdots \int_{\mathbf{r}_N(L)=P[\mathbf{r}_N(0)]} \mathcal{D}\mathbf{r}_N(s) e^{-G/k_BT}, \tag{3.14}$$

where we have imposed periodic boundary conditions and summed over permutations P in contrast to the free boundary conditions implicit in (3.7). The parameter s runs from zero to L, where L is the average circumference around the torus. The effect of inhomogeneities in this circumference, as well as of inhomogeneities in the magnetic field, will be discussed below.

We have, for simplicity, used the free energy for a field parallel to the c axis of a high-T_c superconductor. Although this may be hard to achieve in a toroidal geometry, a similar free energy (with $\tilde{\epsilon}_1 = \epsilon_1$) could be used to model a polycrystalline material, which might be easier to fabricate in the shape of a torus. Alternatively, one could use a single crystal with c axis everywhere parallel to the symmetry axis of the torus. The magnetic field lines would then run parallel to the CuO_2 planes. The free energy would be similar to Eq. (3.3), except with anisotropic "masses" $\tilde{\epsilon}_{1x}$ and $\tilde{\epsilon}_{1y}$, as well as an anisotropic interaction between vortices. Although we have not analyzed this situation in detail, the entangled flux liquid should be qualitatively similar to the more symmetric liquids discussed here, in both toroidal and conventional geometries.

As given by Eq. (3.14), the partition function is identical to the imaginary-time Feynman path integral[29] for the grand canonical partition function of a fluid of interacting bosons in two dimensions with chemical potential $\mu = H\phi_0/4\pi - \epsilon_1$. The trajectories of vortices around the torus are isomorphic to boson world lines. The thermal energy k_BT plays the role of $\hbar$, while the circumference L corresponds to the distance $\beta\hbar$ in the imaginary-time direction. The parameter $\tilde{\epsilon}_1$ plays the role of the boson mass. This analogy, which is summarized in Table I, clearly shows why vortex lines are interesting in high-T_c superconductors: These materials allow us to explore a world of exceptionally light ($\tilde{\epsilon}_1 \ll \epsilon_1$) bosons in which "Planck's constant" (i.e., k_BT) is ten times larger than in conventional materials. Because $\tilde{\epsilon}_1$ tends to zero as $T \rightarrow T_c$ along the H_{c1} curve,[14,15] the boson "mass" can be made arbitrarily small. The importance of vortex line fluctuations is determined in the boson language by the "thermal de Broglie wavelength" Λ_L which translates according to Table I into

$$\Lambda_L \equiv \left[\frac{2\pi\hbar^2\beta}{m}\right]^{1/2} = \left[\frac{2\pi k_B T L}{\tilde{\epsilon}_1}\right]^{1/2}. \tag{3.15}$$

Except for numerical factors, this is the vortex diffusion distance (3.10) with $z = L$. Quantum fluctuations begin to become important for bosons when $\Lambda_L \gtrsim n^{-1/2}$. They dominate the physics for $\Lambda_L \gg n^{-1/2}$, which is equivalent to Eq. (3.13).

Figure 5 shows the expected phase diagram for two-dimensional bosons as a function of "chemical potential" $(H - H_{c1})$ and "temperature" (L^{-1}). The real temperature is held fixed at $T < T_c$. A liquid-gas critical point is absent, because we have assumed a purely repulsive pair potential. The crystalline phase is melted by zero-point motion when the "chemical potential" is small. The meaning of the "crystalline," "normal-liquid," and

TABLE I. Detailed correspondence of the parameters of melted flux liquid with the mass, value of Planck's constant, reciprocal temperature β, and potential of two-dimensional bosons.

Vortex lines	$\tilde{\epsilon}_1$	k_BT	L	$\frac{H\phi_0}{4\pi} - \epsilon_1$	$\frac{\phi_0^2}{8\pi^2\lambda^2} K_0(r/\lambda)$
Two-dimensional bosons	m	$\hbar$	$\beta\hbar$	μ	Boson pair potential

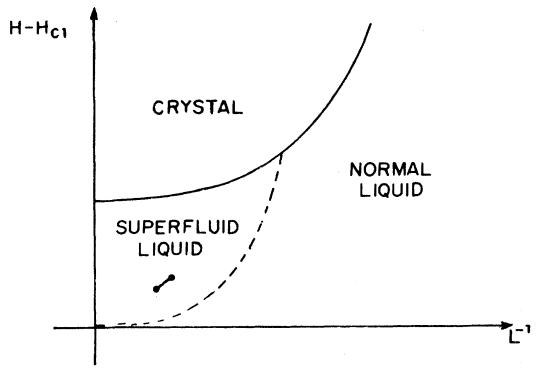

FIG. 5. Schematic phase diagram for vortex lines in a toroidal geometry as a function of "chemical potential" $H-H_{c1}$ and "temperature" L^{-1}. Here, L is the average circumference of the torus in Fig. 4. The line segment in the superfluid phase represents the range of states which might be present inside the torus due to the inhomogeneity of the magnetic field and circumference across a cross sectional area.

"superfluid-liquid" phases for Abrikosov flux lines are illustrated schematically in Fig. 6. The large dots show where the vortex lines pierce, say, the $s=0$ circular cross section of the torus in Fig. 4. The lines show the vortex positions in subsequent cross sections as they traverse the interior of the torus and return to the initial cross section. Figure 6(a) represents a toroidal Abrikosov flux lattice, in which the vortices typically make only small excursions from the sites of a triangular lattice. Figure 6(b) represents a disentangled flux liquid characterized by large excursions of the vortices and no crystalline order in their average positions. In this case, the torus is filled with a liquid of disconnected flux bracelets. Figure 6(c) represents an *entangled* flux liquid in which vortices repeatedly exchange places in a complicated dance as they traverse the torus.

The elegant picture[29] of a superfluid liquid embodied in Fig. 6(c) has been confirmed by some striking computer simulations of Ceperley and Pollock in both two and three dimensions.[30] The beauty of the high-T_c superconductors is that Feynman's artificial imaginary-time variable becomes real and directly accessible to experiments. In its entangled "superfluid" phase, the flux liquid in a torus looks like a mangled spiral of flux lines which only repeats itself after many turns around the torus. A finite fraction of the vortex loops are connected together in such long cycles, which should have important consequences for flux flow resistivity in the presence of pinning. The dashed curve in Fig. 5 is a line of Kosterlitz-Thouless transitions from an entangled flux liquid to a disentangled one. Flux flow resistivity will be suppressed in an entangled flux liquid with a few strong pinning centers, even though there is no shear modulus.

In an actual experiment carried out in a toroidal geometry, both the magnetic field and the circumference will be nonuniform across a circular cross section. This corresponds to an inhomogeneous chemical potential and temperature in the boson system. The physical system can be represented by a line of states, as indicated by the

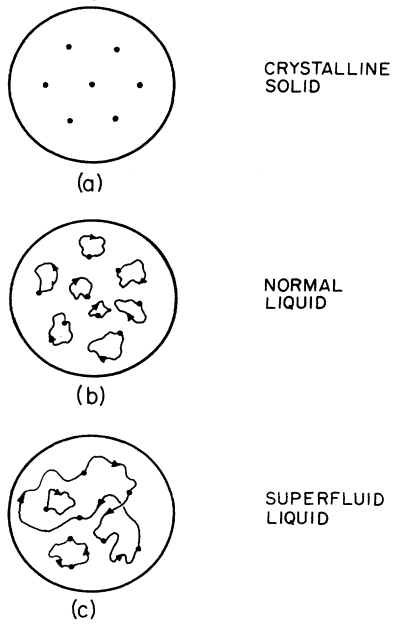

FIG. 6. Trajectories $\mathbf{r}_i(s)$ swept out by vortex lines within a circular cross section of the tours in Fig. 4. All vortices occupy approximately the same relative position within the cross section for all values of s within the Abrikosov flux lattice phase (a). These lines form disentangled flux bracelets in the normal-liquid phase, but may wander appreciably during their circuit around the torus (b). In superfluid phase (c), the flux lines link up, and it may require many circuits around the torus before a flux line returns to its starting point.

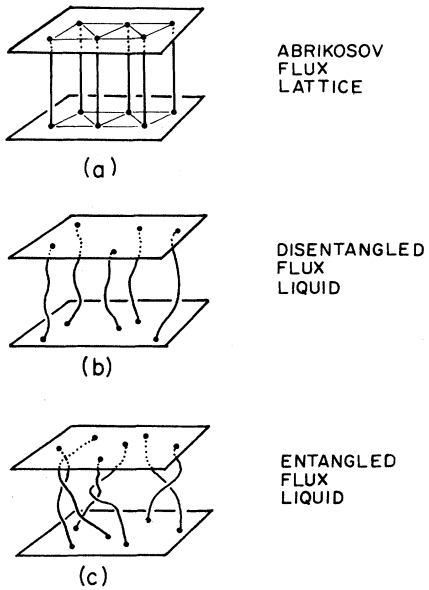

FIG. 7. Analogues of the three phases shown in Fig. 6 for a slab geometry with free, rather than periodic boundary conditions. In contrast to the case of periodic boundary conditions, there is not necessarily a sharp phase transition between (b) and (c).

line segment in Fig. 5. Similar problems arise in real superfluid helium, due to the Earth's gravitational field and temperature inhomogeneities. The result is that the Kosterlitz-Thouless transition discussed above will be spread out over a range of fields and sample thicknesses.

Figure 7 shows the Abrikosov flux lattice, the disentangled flux liquid, and the entangled flux liquid as they would appear in a conventional experimental geometry, with free boundary conditions on the vortex lines. As discussed above, boundary conditions should be irrelevant as the sample thickness tends to infinity. Explicit calculations for the entangled flux liquid in a conventional slab geometry are carried out in Sec. IV. One of the conclusions is that the entangled flux liquid is indistinguishable from a superfluid with periodic boundary conditions whenever (3.13) is satisfied. It is possible, however, that the Kosterlitz-Thouless transition discussed above is smeared out with free boundary conditions, as suggested by Fisher and Lee.[8] It may then be better to speak of entangled and disentangled flux liquid *regimes* instead of phases.[31] The crossover between these two regimes will occur when

$$\xi_z \approx L , \tag{3.16}$$

i.e., when the "thermal de Broglie wavelength" Λ_L is comparable to the vortex line spacing.[2]

IV. VORTEX CORRELATIONS IN AN ENTANGLED LIQUID

Aided by the unifying formalism of the Feynman path integral, we have established an analogy between vortex lines and boson world lines. In this section, we write the Feynman path integral in terms of coherent states[10] in a way which makes this analogy complete. This formalism will provide a way to modify standard boson calculations to produce the structure factor for a flux liquid deep within the entangled regime.

A. Vortex partition function and boson matrix elements

Our starting point is the canonical partition sum associated with Eq. (3.3), i.e.,

$$Z_N = \frac{\Gamma^N}{N!}\int \prod_{i=1}^{N} \mathcal{D}\mathbf{r}_i(z) \exp\left[-\frac{1}{k_B T}\int_0^L dz \left(\sum_{i=1}^{N} \tfrac{1}{2}\tilde{\epsilon}_1 \left|\frac{d\mathbf{r}_i}{dz}\right|^2 + \sum_{i<j} V[\mathbf{r}_i(z)-\mathbf{r}_j(z)]\right)\right]. \tag{4.1}$$

In this equation, and the remainder of this paper, we have adopted Feynman's definition of the path-integral measure $\mathcal{D}\mathbf{r}(z)$.[29] The prefactor Γ^N required for vortex lines in a superconductor will be evaluated below. The path integral (4.1) can be written as

$$Z_N = \frac{\Gamma^N}{N!}\int d^d r_1' \cdots \int d^d r_N' \int d^d r_1 \cdots \int d^d r_N \rho(\mathbf{r}_1', \ldots, \mathbf{r}_N'; \mathbf{r}_1, \ldots, \mathbf{r}_N; L) , \tag{4.2}$$

where $(\Gamma^N/N!)\rho(\mathbf{r}_1', \ldots, \mathbf{r}_N'; \mathbf{r}_1, \ldots, \mathbf{r}_N; L)$ is the conditional partition sum for N vortex lines constrained to be at positions $(\mathbf{r}_1, \ldots, \mathbf{r}_N)$ when $z=0$ and at $(\mathbf{r}_1', \ldots, \mathbf{r}_N')$ when $\mathbf{r}=L$. Upon using a well-known series of transformations,[10,29] we can write $\rho(\mathbf{r}_1', \ldots, \mathbf{r}_N; \mathbf{r}_1, \ldots, \mathbf{r}_N; L)$ as a quantum-mechanical density matrix,

$$\rho(\mathbf{r}_1', \ldots, \mathbf{r}_N'; \mathbf{r}_1, \ldots, \mathbf{r}_N; L) = \langle \mathbf{r}_1', \ldots, \mathbf{r}_N' | e^{-L\hat{\mathcal{H}}/k_B T} | \mathbf{r}_1, \ldots, \mathbf{r}_N \rangle , \tag{4.3}$$

where the "Hamiltonian" $\hat{\mathcal{H}}$ is

$$\hat{\mathcal{H}} = \frac{-(k_B T)^2}{2\tilde{\epsilon}_1}\sum_{i=1}^{N} \nabla_{\mathbf{r}_i}^2 + \tfrac{1}{2}\sum_{i\neq j} V(\mathbf{r}_i - \mathbf{r}_j) . \tag{4.4}$$

The operator $\hat{\mathcal{H}}$ acts on a Hilbert space of states $|\mathbf{r}_1, \ldots, \mathbf{r}_N\rangle$ which is the direct product of single-particle states $|\mathbf{r}_i\rangle$ with normalization

$$\langle \mathbf{r} | \mathbf{r}' \rangle = \delta^{(2)}(\mathbf{r}-\mathbf{r}') . \tag{4.5}$$

The corresponding single-particle momentum eigenfunctions $|\mathbf{p}\rangle$ for a periodic box of area Ω have components

$$\langle \mathbf{r} | \mathbf{p} \rangle = \frac{1}{\sqrt{\Omega}} e^{i\mathbf{r}\cdot\mathbf{p}/\hbar} , \tag{4.6}$$

and normalization

$$\langle \mathbf{p} | \mathbf{p}' \rangle = \delta_{\mathbf{p},\mathbf{p}'} . \tag{4.7}$$

The quantity $e^{-\hat{\mathcal{H}}/k_B T}$ is, of course, the transfer matrix associated with the partition function (4.1). Although only a subset of its eigenfunctions obey boson statistics, it is the ground state (which *must* be bosonic[29]) that matters as $L \to \infty$. In fact, *only bosonic states contribute to the partition sum for finite L as well.* To see this, note first that, according to the Fourier conventions (4.5)–(4.7),

$$\int d^2 r_1 \cdots \int d^2 r_N |\mathbf{r}_1 \cdots \mathbf{r}_N\rangle = \Omega^{N/2} |\mathbf{p}_1 = 0, \ldots, \mathbf{p}_N = 0\rangle , \tag{4.8}$$

where $|\mathbf{p}_1, \ldots, \mathbf{p}_N\rangle = |\mathbf{p}_1\rangle \otimes \cdots \otimes |\mathbf{p}_N\rangle$ is the direct product of one particle momentum eigenstates. The partition function (4.2) thus reduces to a single quantum-mechanical matrix element,

$$Z_N = \frac{(\Gamma\Omega)^N}{N!}\langle \mathbf{p}_1 = 0, \ldots, \mathbf{p}_N = 0 | e^{-L\hat{\mathcal{H}}/k_B T} \times |\mathbf{p}_1 = 0, \ldots, \mathbf{p}_N = 0\rangle , \tag{4.9}$$

formed from states which are symmetrical under particle interchange. If $|\mathbf{p}_1 = 0, \ldots, \mathbf{p}_N = 0\rangle$ is expanded in the complete set of eigenfunctions of $\hat{\mathcal{H}}$, *only symmetric states will appear.* Thus the excited states as well as the ground-state eigenfunctions which contribute to (4.2) will be bosonic for arbitrary L. The usual boson partition function would involve a *trace* over symmetrized momen-

tum eigenstates, instead of the single matrix element which appears in (4.9).[10,29]

We now evaluate the constant Γ. Upon setting $N=1$ in Eq. (4.9), we have

$$Z_1=\Gamma\Omega\langle \mathbf{p}=0|e^{-L\hat{\mathcal{H}}_1/k_BT}|\mathbf{p}=0\rangle =\Gamma\Omega\,, \tag{4.10}$$

where $\hat{\mathcal{H}}_1$ is the one-particle Hamiltonian, $\hat{\mathcal{H}}_1=\hat{\mathbf{p}}^2/2\tilde{\epsilon}_1$. The one-line partition function Z_1 can be evaluated directly by discretizing the path integral with constant-z slices separated by distance b. In this way, we find that

$$\Gamma=\frac{q^{L/b}}{a^2}\,, \tag{4.11a}$$

with

$$q=\frac{2\pi bk_BT}{\tilde{\epsilon}_1a^2}\,, \tag{4.11b}$$

where we have assumed a square lattice (with lattice constant a) of possible vortex positions in each constant-z plane.

B. Coherent-state formalism

As in most calculations with bosons, we shall find it convenient to use the language of second quantization. In this language the Hamiltonian (4.4) takes the form

$$\hat{\mathcal{H}}(\hat{\psi}^\dagger,\hat{\psi})=-\frac{(k_BT)^2}{2\tilde{\epsilon}_1}\int d^2r\,\hat{\psi}^\dagger(\mathbf{r})\nabla^2\hat{\psi}(\mathbf{r})+\tfrac{1}{2}\int d^2r\int d^2r'\hat{\psi}^\dagger(\mathbf{r})\hat{\psi}^\dagger(\mathbf{r}')V(\mathbf{r}-\mathbf{r}')\hat{\psi}(\mathbf{r}')\hat{\psi}(\mathbf{r})\,, \tag{4.12}$$

where $\hat{\psi}(\mathbf{r})$ and $\hat{\psi}^\dagger(\mathbf{r})$ are the usual second-quantized field operators. We now reexpress the path integral in terms of coherent states $|\phi\rangle$, which are defined in terms of the vacuum $|0\rangle$ by

$$|\phi\rangle=\exp\left[\int d^2\mathbf{r}\,\phi(\mathbf{r})\hat{\psi}^\dagger(\mathbf{r})\right]|0\rangle\,. \tag{4.13}$$

The path integral (4.1) is based on position eigenstates, which satisfy the equation $\hat{\mathbf{r}}|\mathbf{r}\rangle=\mathbf{r}|\mathbf{r}\rangle$, where $\hat{\mathbf{r}}$ is the position operator. The new basis satisfies a similar eigenvalue equation, $\hat{\psi}(\mathbf{r})|\phi\rangle=\phi(\mathbf{r})|\phi\rangle$. This change of basis is convenient and natural because we have also switched operators in the Hamiltonian, from $\hat{\mathbf{r}}_i$ and $\hat{\mathbf{p}}_i$ to $\hat{\psi}(\mathbf{r})$ and $\hat{\psi}^\dagger(\mathbf{r})$. By inserting complete sets of coherent states in various constant-z "time" slices, one can derive a coherent state functional integral for the grand canonical density matrix,[10] namely

$$\langle\phi'|e^{-L(\hat{\mathcal{H}}-\mu\hat{N})/k_BT}|\phi\rangle=\int_{\phi(\mathbf{r},0)=\phi(\mathbf{r})}^{\phi(\mathbf{r},L)=\phi'(\mathbf{r})}\mathcal{D}\phi^*(\mathbf{r},z)\mathcal{D}\phi(\mathbf{r},z)\exp\left[\int d^2r\phi^*(\mathbf{r},L)\phi(\mathbf{r},L)\right]$$
$$\times\exp\left\{-\frac{1}{k_BT}\int_0^L dz\left[\int d^2r\phi^*(\mathbf{r},x)\left[k_BT\frac{\partial}{\partial z}-\mu\right]\phi(\mathbf{r},z)+\hat{\mathcal{H}}[\phi^*,\phi]\right]\right\}, \tag{4.14}$$

where the number operator is $\hat{N}=\int d^2r\,\psi^\dagger(\mathbf{r})\psi(\mathbf{r})$. Instead of paths $\mathbf{r}_i(z)$ in configuration space, what we have are "paths" $\phi(\mathbf{r},z)$ in coherent state space.

To obtain the density matrix element (4.9) in the coherent state picture, note first that

$$|\mathbf{p}_1=0,\ldots,\mathbf{p}_N=0\rangle=\frac{1}{\sqrt{N!}}(a_0^\dagger)^N|0\rangle\,,$$

where $a_0^\dagger$ creates a boson with zero momentum and $|0\rangle$ is the vacuum. Thus, we can write using (4.9) that

$$Z_N=\frac{\Gamma^N\Omega^N}{(N!)^2}\langle 0|(a_0)^Ne^{-L\hat{\mathcal{H}}/k_BT}(a_0^\dagger)^N|0\rangle\,. \tag{4.15}$$

It will be convenient to pass to the grand partition function, given by

$$Z_{\rm gr}=\sum_{N=0}^{\infty}e^{L\mu N/k_BT}Z_N\,, \tag{4.16}$$

where, according to Eq. (3.3), we have $\mu=H\phi_0/4\pi-\epsilon_1$. Upon using (4.15), we have

$$Z_{\rm gr}=\sum_{N=0}^{\infty}\left\langle 0\left|\frac{(\sqrt{\Gamma\Omega}a_0)^N}{N!}e^{-L(\hat{\mathcal{H}}-\mu\hat{N})/k_BT}\frac{(\sqrt{\Gamma\Omega}a_0^\dagger)^N}{N!}\right|0\right\rangle=\sum_{N=0}^{\infty}\left\langle 0\left|\frac{(\sqrt{\Gamma\Omega\sigma}a_0)^N}{N!}e^{-L(\hat{\mathcal{H}}-\mu\hat{N})/k_BT}\sigma^{-N}\frac{(\sqrt{\Gamma\Omega\sigma}a_0^\dagger)^N}{N!}\right|0\right\rangle. \tag{4.17}$$

In the last line we have inserted factors of σ, a positive real number whose precise value will be determined later. In terms of the coherent states

$$|\phi(\mathbf{r}_\perp)=\sqrt{\Gamma\sigma}\rangle=\exp\left[\int d^2r_\perp\sqrt{\Gamma\sigma}\hat{\psi}^\dagger(\mathbf{r}_\perp)\right]|0\rangle=\sum_{N=0}^{\infty}\frac{(\sqrt{\Gamma\Omega\sigma}a_0^\dagger)^N}{N!}|0\rangle\,, \tag{4.18}$$

so the partition function becomes

$$Z_{\rm gr}=\langle\phi(\mathbf{r}_\perp)=\sqrt{\Gamma\sigma}\,|\,e^{-L(\hat{\mathcal{H}}-\tilde{\mu}\hat{N})/k_BT}\,|\,\phi(\mathbf{r}_\perp)=\sqrt{\Gamma\sigma}\rangle\,, \tag{4.19}$$

where we have used the fact that the Hamiltonian does not connect states with different particle number. This expression contains a "renormalized" chemical potential $\tilde{\mu}$ satisfying

$$\tilde{\mu}=\mu-\frac{k_BT}{L}\ln\sigma\,. \tag{4.20}$$

We can now apply (4.14) to write this expression as a functional integral,

$$Z_{\rm gr}=e^{\Gamma\Omega\sigma}\int_{\phi(\mathbf{r},0)=\sqrt{\Gamma\sigma}}^{\phi(\mathbf{r},L)=\sqrt{\Gamma\sigma}}\mathcal{D}\phi^*(\mathbf{r}_\perp,z)\mathcal{D}\phi(\mathbf{r}_\perp,z)e^{-S[\phi^*,\phi]}\,, \tag{4.21}$$

where the "action" S is given by

$$S[\phi^*,\phi]=\frac{1}{k_BT}\int_0^L dz\int d^2r_\perp\,\phi^*(\mathbf{r}_\perp,z)\left[k_BT\frac{\partial}{\partial z}-\frac{(k_BT)^2\nabla^2}{2\tilde{\epsilon}_1}-\tilde{\mu}\right]\phi(\mathbf{r}_\perp,z)$$
$$+\frac{1}{2k_BT}\int_0^L dz\int d^2x\int d^2y\,V(\mathbf{x}-\mathbf{y})\,|\,\phi(\mathbf{x},z)\,|^2\,|\,\phi(\mathbf{y},z)\,|^2\,. \tag{4.22}$$

It is easily shown using similar manipulations that the density of flux lines (1.1) is just

$$n(\mathbf{r}_\perp,z)=\langle\,|\,\phi(\mathbf{r}_\perp,z)\,|^2\rangle\,, \tag{4.23}$$

where the average is sampled with probability $\propto e^{-S[\phi^*,\phi]}$.

The vortex line partition function (4.21) differs significantly from the corresponding boson coherent-state partition function[10] only at $z=0$ and $z=L$, where the field ϕ is constrained to have the value $\sqrt{\Gamma\sigma}$ for all $\mathbf{r}$. For the boson partition function, ϕ can take on any values on these boundaries as long as it is periodic in z.

C. Mean-field theory

In the mean-field approximation, we simply minimize (4.22) by letting $\phi(x,\tau)=\phi_c$ be constant. All the derivative terms vanish, leaving

$$k_BTS[\phi_c^*,\phi_c]=\int_0^L dz\int d^2r(-\tilde{\mu}\,|\,\phi_c\,|^2+\tfrac{1}{2}V_0\,|\,\phi_c\,|^4)\,, \tag{4.24}$$

where $V_0\equiv\int d^2x\,V(\mathbf{x})$. Using the familiar Landau potential appearing in the integrand, we can construct a simple picture of the transition which occurs when $\tilde{\mu}$ changes sign. The minima of the Landau potential are at

$$\phi_c=0,\quad\text{for }\tilde{\mu}<0\,, \tag{4.25}$$

$$\phi_c=\left(\frac{\tilde{\mu}}{V_0}\right)^{1/2},\quad\text{for }\tilde{\mu}>0\,. \tag{4.26}$$

The line $\tilde{\mu}=0$ is a phase boundary. In the phase of negative $\tilde{\mu}$ the boson density $n=|\,\phi\,|^2$ is zero. But for positive chemical potential, $n=\tilde{\mu}/V_0$. When translated into superconductor language, these results describe vortex lines in a toroidal geometry.

This mean-field solution must, however, respect the boundary conditions associated with the open geometry, i.e., $\phi(\mathbf{r}_\perp,0)=\phi(\mathbf{r}_\perp,L)=\sqrt{\Gamma\sigma}$. The mean-field density $n=\tilde{\mu}/V_0$ must also equal $\Gamma\sigma$, which allows us to fix σ,

$$\sigma=\frac{n}{\Gamma}=\frac{N}{Z_1}\,, \tag{4.27}$$

where the last equality follows from (4.10). The "renormalized" chemical potential (4.20) is thus

$$\tilde{\mu}=\mu-\frac{k_BT}{L}\ln\frac{N}{Z_1}\,. \tag{4.28}$$

The correction to $\mu=H\phi_0/4\pi-\epsilon_1$ leads to a downward renormalization of H_{c1}, whose physical significance will be discussed in Sec. V C.

D. Vortex line correlations

Thus far, we have found no essential differences between the bosons with open boundary conditions of interest to us here and conventional bosons with periodic boundary conditions. Differences do appear, however, in correlation functions evaluated for finite L. We first review how these correlations are calculated for conventional bosons,[11] and then describe the changes which occur when open boundary conditions are taken into account.

The complex field $\phi(\mathbf{r},z)$ is written in terms of two new real variables, the density $n(\mathbf{r},z)$ and the phase $\theta(\mathbf{r},z)$,

$$\phi(\mathbf{r},z)\equiv\sqrt{n(\mathbf{r},z)}e^{i\theta(\mathbf{r},z)}\,. \tag{4.29}$$

The measure takes the simple form (up to unimportant constant factors)

$$\mathcal{D}\phi^*(\mathbf{r},z)\mathcal{D}\phi(\mathbf{r},z)=\mathcal{D}n(\mathbf{r},z)\mathcal{D}\theta(\mathbf{r},z)\,. \tag{4.30}$$

For simplicity, we replace $V(\mathbf{r}-\mathbf{r}')$ by a contact potential $V_0\delta^{(2)}(\mathbf{r}-\mathbf{r}')$ in (4.22), and replace the superconducting parameters by bosonic ones using Table I. There is no renormalization of μ for bosons with periodic boundary con-

ditions. The action now reads

$$S^{\text{boson}}=\frac{1}{\hbar}\int_0^{\beta\hbar}dz\int d^2r\left[\phi^*\hbar\frac{\partial\phi}{\partial z}+\frac{\hbar^2}{2m}|\nabla\phi|^2-\mu|\phi|^2+\tfrac{1}{2}V_0|\phi|^4\right], \tag{4.31}$$

or using (4.29),

$$S^{\text{boson}}=\frac{1}{\hbar}\int_0^{\beta\hbar}dz\int d^2r\left[i\hbar n\frac{\partial\theta}{\partial z}+\frac{\hbar^2(\nabla n)^2}{8mn}+\frac{\hbar^2 n(\nabla\theta)^2}{2m}-\mu n+\tfrac{1}{2}V_0 n^2\right], \tag{4.32}$$

where total derivative terms have vanished because of the periodic boundary conditions. We now define $\pi\equiv n-n_0$, where $n_0=\mu/V_0$ is the (boson) mean-field magnitude, and expand to quadratic order in π and θ:

$$S^{\text{boson}}\approx\frac{1}{\hbar}\int_0^{\beta\hbar}dz\int d^2r\left[i\hbar n_0\frac{\partial\theta}{\partial z}+i\hbar\pi\frac{\partial\theta}{\partial z}+\frac{\hbar^2(\nabla\pi)^2}{8mn_0}+\frac{n_0\hbar^2(\nabla\theta)^2}{2m}+\tfrac{1}{2}V_0\pi^2-\frac{\mu^2}{2V_0}\right]. \tag{4.33}$$

The integral of $in_0\partial\theta/\partial z$ vanishes provided that θ is single valued.

Let us expand the fields in Fourier series:

$$\theta(\mathbf{r},z)=\frac{1}{\sqrt{\beta\hbar\,\Omega}}\sum_{\mathbf{k},\omega}e^{i\omega z+i\mathbf{k}\cdot\mathbf{r}}\theta(\mathbf{k},\omega), \tag{4.34}$$

and similarly for π. The sum is over momenta $\mathbf{k}$ satisfying periodic boundary conditions and the Matsubara frequencies $\omega_n=2\pi n/\beta\hbar$.[32] The action (4.33) is diagonal in these Fourier modes,

$$S^{\text{boson}}=\tfrac{1}{2}\sum_{\mathbf{k},\omega}\Upsilon^\dagger(\mathbf{k},\omega)G^{-1}(\mathbf{k},\omega)\Upsilon(\mathbf{k},\omega)+\text{const}, \tag{4.35}$$

where $\Upsilon(\mathbf{k},\omega)$ is the column vector

$$\Upsilon(\mathbf{k},\omega)=\begin{bmatrix}\theta(\mathbf{k},\omega)\\ \pi(\mathbf{k},\omega)\end{bmatrix}, \tag{4.36}$$

and the coefficient matrix is

$$G^{-1}(\mathbf{k},\omega)=\begin{bmatrix}\dfrac{n_0\hbar k^2}{m} & -\omega\\ \omega & \dfrac{V_0}{\hbar}+\dfrac{\hbar k^2}{4mn_0}\end{bmatrix}. \tag{4.37}$$

Since the functional integrals are just Gaussians, it can easily be shown that the correlations are given by the inverse of the coefficient matrix

$$\langle\Upsilon(\mathbf{k},\omega)\Upsilon^\dagger(\mathbf{k}',\omega')\rangle=G(\mathbf{k},\omega)\delta_{\mathbf{k},\mathbf{k}'}\delta_{\omega,\omega'}. \tag{4.38}$$

Consider, in particular, the density correlation function,

$$S(\mathbf{r},z)\equiv\langle n(\mathbf{r},z)n(\mathbf{0},0)\rangle-n_0^2. \tag{4.39}$$

The structure function is just the Fourier transform

$$\begin{aligned}S(\mathbf{k},\omega)&=\int_0^{\beta\hbar}dz\int d^2r\,e^{-i\omega z-i\mathbf{k}\cdot\mathbf{r}}S(\mathbf{r},z)\\&=\langle\pi(\mathbf{k},\omega)\pi^*(\mathbf{k},\omega)\rangle\\&=\frac{n_0\hbar k^2/m}{\omega^2+\varepsilon^2(k)/\hbar^2},\end{aligned} \tag{4.40}$$

where $\varepsilon(k)$ is the Bogoliubov spectrum

$$\varepsilon(k)=\left[\left(\frac{\hbar^2k^2}{2m}\right)^2+\frac{\mu\hbar^2k^2}{m}\right]^{1/2}. \tag{4.41}$$

Equation (4.38) is also the structure factor for vortex lines in a toroidal geometry, provided we use Table I and identify $\mathbf{k}$ and ω with $q_\perp$ and q_z in Eq. (1.2).

Now we are faced with the task of modifying this calculation for the case of an open geometry. The action to quadratic order is still given by Eq. (4.33), provided we substitute superconducting parameters for boson ones and let $\mu\rightarrow\tilde{\mu}$. However, both π and θ must be zero at $z=0$ and $z=L$, to satisfy the boundary conditions in (4.21). Inserting a δ functional enforces this constraint:

$$\langle\Upsilon(1)\Upsilon^\dagger(2)\rangle=\frac{\int\mathcal{D}\Upsilon(\mathbf{r}_\perp,z)e^{-S}\Upsilon(1)\Upsilon^\dagger(2)\prod_{\mathbf{r}_\perp}\delta[\Upsilon(\mathbf{r}_\perp,z=0)]}{\int\mathcal{D}\Upsilon(\mathbf{r}_\perp,z)e^{-S}\prod_{\mathbf{r}_\perp}\delta[\Upsilon(\mathbf{r}_\perp,z=0)]}, \tag{4.42}$$

where $\Upsilon(1)=\Upsilon(\mathbf{r}_{\perp,},z_1)$, etc. As before, the functional integrals are over all π and θ satisfying periodic boundary conditions, in z, so that the Fourier representation (4.34) is still valid. The δ functional can then be transformed into a functional integral over a row vector field $\lambda^T(\mathbf{r}_\perp)=[\lambda_\theta(\mathbf{r}_\perp),\lambda_\pi(\mathbf{r}_\perp)]$,

$$\langle\Upsilon(1)\Upsilon^\dagger(2)\rangle=\frac{\int\mathcal{D}\lambda\int\mathcal{D}\Upsilon e^{-S}\Upsilon(1)\Upsilon(2)\exp\left[i\int d^2r_\perp\lambda^T(\mathbf{r}_\perp)\Upsilon(\mathbf{r}_\perp,z=0)\right]}{\int\mathcal{D}\lambda\int\mathcal{D}\Upsilon e^{-S}\exp\left[i\int d^2r_\perp\lambda^T(\mathbf{r}_\perp)\Upsilon(\mathbf{r}_\perp,z=0)\right]}. \tag{4.43}$$

Equation (4.43) can also be written as

$$\langle \Upsilon(1)\Upsilon^{\dagger}(2)\rangle = \frac{\int \mathcal{D}\lambda \left\langle \Upsilon(1)\Upsilon^{\dagger}(2)\exp\left[i\int d^2r_{\perp}\lambda^{T}(\mathbf{r}_{\perp})\Upsilon(\mathbf{r}_{\perp},z=0)\right]\right\rangle_0}{\int \mathcal{D}\lambda \left\langle \exp\left[i\int d^2r_{\perp}\lambda^{T}(\mathbf{r}_{\perp})\Upsilon(\mathbf{r}_{\perp},z=0)\right]\right\rangle_0}, \tag{4.44}$$

where we have defined $\langle\cdots\rangle_0$ to mean averaging with respect to e^{-S} over all Υ satisfying periodic boundary conditions,

$$\left\langle \Upsilon(1)\Upsilon^{\dagger}(2)\exp\left[i\int d^2r_{\perp}\lambda^{T}(\mathbf{r}_{\perp})\Upsilon(\mathbf{r}_{\perp},z=0)\right]\right\rangle_0 \equiv \frac{\int \mathcal{D}\Upsilon\left[\Upsilon(1)\Upsilon^{\dagger}(2)\exp\left[i\int d^2r_{\perp}\lambda^{T}(\mathbf{r}_{\perp})\Upsilon(\mathbf{r}_{\perp},z=0)\right]\right]e^{-S}}{\int \mathcal{D}\Upsilon e^{-S}}. \tag{4.45}$$

These Gaussian averages are easily evaluated in Fourier space. We have

$$\left\langle \exp\left[i\int d^2r_{\perp}\lambda^{T}(\mathbf{r}_{\perp})\Upsilon(\mathbf{r}_{\perp},z=0)\right]\right\rangle_0 = \left\langle \exp\left[i\sum_{\mathbf{k},\omega}\lambda^{\dagger}(\mathbf{k})\Upsilon(\mathbf{k},\omega)\right]\right\rangle_0 = \exp\left[-\tfrac{1}{2}\sum_{\mathbf{k}}\lambda^{\dagger}(\mathbf{k})\sum_{\omega}G(\mathbf{k},\omega)\lambda(\mathbf{k})\right], \tag{4.46}$$

and

$$\left\langle \Upsilon(\mathbf{k},\omega)\Upsilon^{\dagger}(\mathbf{k}',\omega')\exp\left[i\sum_{\mathbf{q},\omega}\lambda^{\dagger}(\mathbf{q})\Upsilon(\mathbf{q},\omega)\right]\right\rangle_0 = [G(\mathbf{k},\omega)\delta_{\mathbf{k},\mathbf{k}'}\delta_{\omega,\omega'} - G(\mathbf{k},\omega)\lambda(\mathbf{k})\lambda^{\dagger}(\mathbf{k}')G(\mathbf{k}',\omega')] \times\exp\left[-\tfrac{1}{2}\sum_{\mathbf{q}}\lambda^{\dagger}(\mathbf{q})\sum_{\omega}G(\mathbf{q},\omega)\lambda(\mathbf{q})\right]. \tag{4.47}$$

Substituting these expressions into the functional integrals in (4.44) we obtain finally

$$\langle \Upsilon(\mathbf{k},\omega)\Upsilon^{\dagger}(\mathbf{k}',\omega')\rangle = G(\mathbf{k},\omega)\delta_{\mathbf{k},\mathbf{k}'}\delta_{\omega,\omega'} - G(\mathbf{k},\omega)\left[\sum_{\nu_n}G(\mathbf{k},\nu_n)\right]^{-1}G(\mathbf{k},\omega')\delta_{\mathbf{k},\mathbf{k}'}. \tag{4.48}$$

The second term on the right is a correction to Popov's result[11] (4.38) for the Bose gas, and represents the effects of free boundary conditions. A simple consistency check on this result can be obtained by summing over ω and ω'. The right side vanishes, proving that

$$\langle \Upsilon(\mathbf{k},z=0)\Upsilon^{\dagger}(\mathbf{k}',z=0)\rangle = \langle \Upsilon(\mathbf{k},z=L)\Upsilon^{\dagger}(\mathbf{k}',z=L)\rangle = 0.$$

This must be so, since no fluctuations are allowed at the boundary.

The sum in (4.48) is over the Matsubara frequencies $\nu_n = 2\pi n/L$, and yields a diagonal matrix, which can easily be inverted,

$$\left[\sum_{\nu_n}G(\mathbf{k},\nu_n)\right]^{-1} = \frac{\tanh[L\varepsilon(k)/2k_BT]}{[L\varepsilon(k)/2k_BT]}G^{-1}(\mathbf{k},0). \tag{4.49}$$

Thus

$$\langle \Upsilon(\mathbf{k},\omega)\Upsilon^{\dagger}(\mathbf{k}',\omega')\rangle = G(\mathbf{k},\omega)\delta_{k,k'}\delta_{\omega,\omega'} - \frac{\tanh[L\varepsilon(k)/2k_BT]}{[L\varepsilon(k)/2k_BT]}G(\mathbf{k},\omega)G^{-1}(\mathbf{k},0)G(\mathbf{k},\omega')\delta_{\mathbf{k},\mathbf{k}'}. \tag{4.50}$$

This result indicates that, as expected, the corrections to the results appropriate to bosons with free boundary conditions become negligible as $L\to\infty$.

We can now discuss the structure function of a melted flux liquid in more detail. Using the notation of Eq. (1.2) (i.e., $\mathbf{k}\to\mathbf{q}_{\perp}$, $\omega\to q_z$), we rewrite (4.40) as

$$S(\mathbf{q}_{\perp},q_z) = \frac{nk_BTq_{\perp}^2/\tilde{\epsilon}_1}{q_z^2+\varepsilon^2(q_{\perp})/(k_BT)^2}, \tag{4.51}$$

where, in terms of superconducting parameters, the Bogoliubov spectrum (4.41) becomes

$$\frac{\varepsilon(q_{\perp})}{k_BT} = \left[\left(\frac{k_BTq_{\perp}^2}{2\tilde{\epsilon}_1}\right)^2 + \frac{\tilde{\mu}q_{\perp}^2}{\tilde{\epsilon}_1}\right]^{1/2}. \tag{4.52}$$

Upon carrying out the partial Fourier transform of Eq. (4.51), we see that density fluctuations in the line liquid do indeed fall off exponentially with z as indicated in Eq. (1.4), at a rate given by Eq. (1.5), with

$$\xi_{\parallel}(q_{\perp}) = \left[\left(\frac{k_BTq_{\perp}^2}{2\tilde{\epsilon}_1}\right)^2 + \frac{\tilde{\mu}q_{\perp}^2}{\tilde{\epsilon}_1}\right]^{-1/2}. \tag{4.53}$$

Note that $\xi_{\parallel}(q_{\perp})\to\infty$ as $q_{\perp}\to 0$, so that long-wavelength fluctuations die off very slowly. The $q_{\perp}=0$ Fourier mode persists forever because the number of flux lines in any constant-z cross section is conserved.

The most important decay modes are those with wave vectors $q_{\perp}\sim(n)^{1/2}\sim 1/d$, i.e., with $q_{\perp}^{-1}$ comparable to the vortex line spacing. This range of wave vectors occurs when the two terms in the denominator of (4.53) are comparable. Thus we have

$$\xi_{\parallel}(q_{\perp}\sim 1/d) \sim \frac{\tilde{\epsilon}_1}{2k_BTn} = \xi_z, \tag{4.54}$$

where ξ_z is the correlation length defined in Eq. (3.12). As discussed in Sec. III, this distance is just the spacing between vortex collisions. Because $n \approx \tilde{\mu}/V_0$, ξ_z diverges

$$\xi_z \sim 1/\tilde{\mu} , \tag{4.55}$$

as $H \rightarrow H_{c1}$ from above in mean-field theory.

Although these results were obtained in the Bogoliubov approximation appropriate to a dilute gas of vortex lines, we believe their qualitative features are more general. Equation (4.51), for example, is just the Wick rotation ($\omega \rightarrow iq_z$) of the Bogoliubov approximation for the dynamical structure factor $S(\mathbf{q}_\perp,\omega)$ of a two-dimensional superfluid. It should be possible to obtain this correlation function for a dense vortex liquid near H_{c2} by a similar Wick rotation of $S(\mathbf{q}_\perp,\omega)$ of a dense superfluid. This quantity will be dominated at low temperatures (i.e., as $L \rightarrow \infty$ in the vortex liquid) by peaks at phonon-roton excitation spectrum, which leads to Eq. (1.4) in the "single-mode" approximation. Our expectations for correlations in dense flux liquids are summarized in Fig. 2.

V. RENORMALIZATION GROUP FOR LINE LIQUIDS NEAR H_{c1}

To analyze the dilute regime near H_{c1}, we return to our original path integral expression for the partition function and develop a perturbation theory for it. The formalism of this section utilizes yet another physical analogy: the path integral partition function for vortex lines also resembles the Edwards model for interacting polymers.[33] We can think of a vortex line $\mathbf{r}_i(z)$ as a two-dimensional polymer, where z plays the role of a monomer index. Unlike polymers, the vortex lines are not self-avoiding: they are true random walks in two dimensions. This makes the perturbation theory much simpler than it is for interacting polymers. The interactions, moreover, only occur between different "polymers" at equal values of the monomer index z.

In this section, we will set $v(\mathbf{r}) \equiv V(\mathbf{r})/k_BT$, subsuming k_BT into the definition of the interaction. The Fourier transform of this Bessel function interaction [see Eq. (3.2)] gives

$$\tilde{v}(\mathbf{k}) = \frac{\phi_0^2}{4\pi k_BT} \frac{1}{1+k^2\lambda^2} . \tag{5.1}$$

As we shall see below, the behavior near H_{c1} is "universal," so it should be insensitive to the precise form of the potential. To simplify the renormalization-group analysis, we are thus free to introduce an approximate pseudopotential:

$$\tilde{v}(\mathbf{k}) \approx \begin{cases} \phi_0^2/4\pi k_BT, & k < \Lambda , \\ 0, & k > \Lambda . \end{cases} \tag{5.2}$$

What we have done here is approximate $\tilde{v}(\mathbf{k})$ by its value for $\mathbf{k}=0$ out to some cutoff $\Lambda \approx 1/\lambda$, outside which it is zero. The Hamiltonian now takes the form

$$H/k_BT = \tfrac{1}{2}K\int_0^L dz \sum_{i=1}^{N} \left| \frac{d\mathbf{r}_i}{dz} \right|^2 + v_0 \sum_{i<j} \int_0^L dz \frac{1}{\Omega} \sum_{k<\Lambda} e^{i\mathbf{k}\cdot[\mathbf{r}_i(z)-\mathbf{r}_j(z)]} . \tag{5.3}$$

Only three parameters remain in the Hamiltonian: $K \equiv \tilde{\epsilon}_1/k_BT$, $v_0 \equiv \phi_0^2/4\pi k_BT$, and $\Lambda \approx 1/\lambda$. The coupling K should not be confused with the tilt modulus of Sec. II. Let us generalize to vortex lines in $d+1$ dimensions, so that the $\mathbf{r}_i$ are d-dimensional vectors. A simple rescaling reduces the number of parameters to two, the cutoff Λ and a natural coupling constant v_0K with dimensions of (length)$^{d-2}$. This suggests that $d=2$ is the critical dimension below which the interaction should be a relevant variable.[34]

We will first construct a diagrammatic formalism to evaluate the vortex partition function, and derive renormalization-group recursion relations. The model (5.3) turns out to be asymptotically free in dimension $d=2$: The dimensionless coupling v_0K is driven to zero at long wavelengths. We then apply the recursion relations to a flux liquid near H_{c1} with $L=\infty$, and iterate them deep into the entangled regime. This mapping enables us to emphasize the random-walk interpretation rather than the quantum-mechanical analogy of Sec. IV. We "match" onto the results of Sec. IV, producing the constitutive relation and vortex correlation function near H_{c1}.

A. Perturbation theory

Setting $N=1$ in Eq. (4.2) yields the one-vortex partition function

$$Z_1 = \Gamma \int d^dR \int d^dR_0 \, G(\mathbf{R},\mathbf{R}_0;L) , \tag{5.4}$$

where

$$G(\mathbf{R},\mathbf{R}_0;L) \equiv G(\mathbf{R}-\mathbf{R}_0,L)$$

$$\equiv \int_{\mathbf{r}(0)=\mathbf{R}_0}^{\mathbf{r}(L)=\mathbf{R}} \mathcal{D}\mathbf{r}(z) \exp\left[-\tfrac{1}{2}K\int_0^L dz \left| \frac{d\mathbf{r}}{dz} \right|^2 \right] . \tag{5.5}$$

Given some initial position $\mathbf{R}_0$, $G(\mathbf{R},\mathbf{R}_0;L)$ is just the probability that a vortex line of length L will random walk to $\mathbf{R}$ at the other side of the sample. The path integral is normalized such that[35]

$$G(\mathbf{R};L) = \left(\frac{K}{2\pi L} \right)^{d/2} e^{-(1/2)KR^2/L} , \tag{5.6}$$

or in Fourier space

$$G(\mathbf{k},L) \equiv \int d^dR \, e^{-i\mathbf{k}\cdot\mathbf{R}} G(\mathbf{R},L) = e^{-(1/2)k^2L/K} . \tag{5.7}$$

This particular choice of measure for the path integral (5.5) gives the Green's function the normalization $\int d^dR \, G(\mathbf{R},L) = 1$.

The two-vortex Green's function is defined similarly

$$G_2(\mathbf{R}_1',\mathbf{R}_2';\mathbf{R}_1,\mathbf{R}_2;L)=\int_{\mathbf{r}_1(0)=\mathbf{R}_1}^{\mathbf{r}_1(L)=\mathbf{R}_1'}\mathcal{D}\mathbf{r}_1(z)\int_{\mathbf{r}_2(0)=\mathbf{R}_2}^{\mathbf{r}_2(L)=\mathbf{R}_2'}\mathcal{D}\mathbf{r}_2(z)\exp\left[-\tfrac{1}{2}K\int_0^L dz\left|\frac{d\mathbf{r}_1}{dz}\right|^2-\tfrac{1}{2}K\int_0^L dz\left|\frac{d\mathbf{r}_2}{dz}\right|^2-\int_0^L dz\,v[\mathbf{r}_1(z)-\mathbf{r}_2(z)]\right]. \tag{5.8}$$

Expanding the exponential of the interaction as a series in $v(\mathbf{r}_1-\mathbf{r}_2)$, we obtain

$$G_2(\mathbf{R}_1',\mathbf{R}_2';\mathbf{R}_1,\mathbf{R}_2;L)=G(\mathbf{R}_1'-\mathbf{R}_1,L)G(\mathbf{R}_2'-\mathbf{R}_2,L)-\int_0^L dz\int d^dx\int d^dy\,G(\mathbf{R}_1'-\mathbf{x},L-z)G(\mathbf{x}-\mathbf{R}_1,z)v(\mathbf{x}-\mathbf{y})\times G(\mathbf{R}_2'-\mathbf{y},L-z)G(\mathbf{y}-\mathbf{R}_2,z)+O(v^2). \tag{5.9}$$

The first term of the expansion represents two lines wandering across the sample without ever interacting. In the second term, we have used the factorization property of path integrals.[35] That is, since the lines interact only at height z in the sample, we can regard each line as *two* noninteracting random walks of lengths z and $L-z$ set end to end. The whole sum can be represented diagrammatically as the infinite sum of "ladder" diagrams shown in Fig. 8. Every power of the interaction v adds another "rung" to the ladder. Higher-order Green's functions can be defined similarly.

Each diagram for the general Fourier-transformed N-vortex Green's function

$$G_N(\mathbf{k}_1,\ldots,\mathbf{k}_N;\mathbf{q}_1,\ldots,\mathbf{q}_N;L)\equiv\int d^dR_1'\cdots\int d^dR_N'\int d^dR_1\cdots\int d^dR_N e^{-i\mathbf{k}_1\cdot\mathbf{R}_1'-\cdots-i\mathbf{k}_N\cdot\mathbf{R}_N'}\times e^{i\mathbf{q}_1\cdot\mathbf{R}_1+\cdots+i\mathbf{q}_N\cdot\mathbf{R}_N}G_N(\mathbf{R}_1',\ldots,\mathbf{R}_N';\mathbf{R}_1,\ldots,\mathbf{R}_N;L) \tag{5.10}$$

is composed of N solid lines whose ends are labeled with the external momenta $\mathbf{k}_1,\ldots,\mathbf{k}_N$ and $\mathbf{q}_1,\ldots,\mathbf{q}_N$. It also contains I dotted interaction lines, each one transferring momentum between a pair of solid lines at some length z. Each solid line is split up by the interactions into segments whose lengths total L. The rules of calculation are as follows:

(1) Assign momenta to all segments and interaction lines, conserving momentum at each vertex.

(2) A segment of length z and carrying momentum $\mathbf{k}$ becomes $G(\mathbf{k},z)$.

(3) An interaction line transferring momentum $\mathbf{k}$ becomes $-\tilde{v}(\mathbf{k})$.

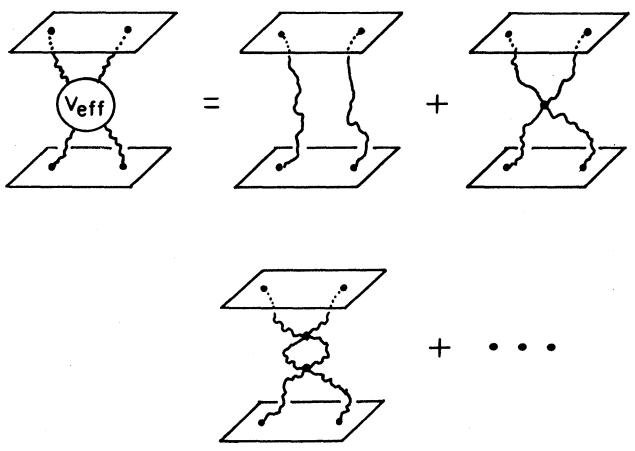

FIG. 8. Diagrams which determine the effective interaction between vortex lines due to repeated collisions.

(4) Integrate over all unconstrained momenta.

(5) Include a factor of Ω and a momentum-conserving δ function for each connected component. This leads to an overall factor of Ω^{N-I+L}, where N is the number of solid lines, I the number of interaction lines, and L the loop number. The number of loops is also the number of unconstrained momenta.

(6) As drawn in the diagram, the interaction lines are ordered in z. We integrate over all possible configurations that preserve this ordering. In other words, if the interaction lines are at $z_1<z_2<\cdots<z_I$, we integrate using

$$\int_0^L dz_1\int_{z_1}^L dz_2\cdots\int_{z_{I-1}}^L dz_I\,.$$

To obtain the N-vortex partition function, we do not have to compute (5.10) in its full generality. We need only evaluate diagrams whose external momenta are all zero, since

$$Z_N=\frac{\Gamma^N}{N!}G_N(\mathbf{k}_1=\cdots=\mathbf{k}_N=0;\mathbf{q}_1=\cdots=\mathbf{q}_N=0;L)\,. \tag{5.11}$$

Furthermore, we need only evaluate connected diagrams; any disconnected diagram can be factored into its connected components. Hence the functions G_N^c (computed using only connected diagrams) are the quantities of interest. The grand partition function can be expressed compactly as

$$\ln Z_{\rm gr}=\sum_{N=1}^{\infty}\frac{e^{N\mu L/k_BT}\Gamma^N}{N!}G_N^c(\mathbf{k}_i=0;\mathbf{q}_i=0;L)\,, \tag{5.12}$$

which is a generalization of the Mayer cluster expansion.[36] The zero-momentum connected Green's function G_m^c corresponds to the m-particle Mayer cluster integral. The first cluster integral is just $G_1^c=\Omega$. The second clus-

ter integral is given by

$$G_2^c = -v_0 L\Omega + v_0^2 \Omega \int_{p<\Lambda} \frac{d^d p}{(2\pi)^d} \int_0^L dz \int_z^L dz' G_0^2(\mathbf{p}, z'-z) + O(v_0^3) , \tag{5.13}$$

where we have now employed the pseudopotential (5.2).

B. Renormalization-group recursion relations

Our perturbation theory is only useful for small v. To compute quantities for large v, we could try summing an infinite set of diagrams to derive results valid beyond the perturbative regime. An equivalent and more systematic approach is to use the renormalization group. We define the renormalized coupling constant associated with the diagrams of Fig. 8 as follows:

$$v' = v_0 \left[1 - \frac{v_0}{L} \int_{\Lambda e^{-\delta} < p < \Lambda} \frac{d^d p}{(2\pi)^d} \int_0^L dz \int_z^L dz' G_0^2(\mathbf{p}, z'-z) \right] \approx v_0 \left[1 - \delta \frac{v_0}{L} K_d \Lambda^d \frac{\Lambda^2 L/K - 1 + e^{-\Lambda^2 L/K}}{(\Lambda^2/K)^2} \right] , \tag{5.14}$$

where $K_d = S_d/(2\pi)^d$ and $S_d = 2\pi^{d/2}/\Gamma(d/2)$ is the surface area of a d-dimensional unit sphere. Simultaneously substituting v' for v_0 in (5.13) and changing the momentum integral cutoff from Λ to $\Lambda e^{-\delta}$ leaves the cluster integral G_2^c invariant to first order in δ. Recall that $\Lambda \sim \lambda^{-1}$ in our model.

We now rescale the momentum $\mathbf{p} \rightarrow \mathbf{p} e^{\delta}$, restoring the cutoff to its original value. We also rescale $z \rightarrow z e^{-\zeta\delta}$. In terms of the dimensionless parameter $\bar{v} \equiv v_0 K \Lambda^{d-2}$, the recursion relation for the coupling constant becomes

$$\frac{d\bar{v}}{dl} = \epsilon \bar{v} - \bar{v}^2 K_d \frac{\Lambda^2 L/K - 1 + e^{-\Lambda^2 L/K}}{\Lambda^2 L/K} , \tag{5.15}$$

where $\epsilon \equiv 2 - d$ is the deviation from the critical dimension.

In the large L limit, this simplifies to

$$\frac{d\bar{v}}{dl} = \epsilon \bar{v} - K_d \bar{v}^2 . \tag{5.16}$$

For $\epsilon > 0$ there is a nontrivial fixed point at $\bar{v}^* = \epsilon/K_d$. In the case of physical interest, however, $\epsilon = 0$, and the theory is asymptotically free,

$$\bar{v}(l) = \frac{\bar{v}(0)}{1 + \bar{v}(0) K_2 l} . \tag{5.17}$$

Since the renormalized coupling constant tends to zero at long wavelengths, perturbation theory should become better and better as $l \rightarrow \infty$.

The recursion relations for K and L are just those given by naive scaling,

$$\frac{dK}{dl} = (2 - \zeta) K , \qquad \frac{dL}{dl} = -\zeta L . \tag{5.18}$$

We shall also need the recursion relation for chemical potential per unit length in the grand partition function. The product μL remains fixed under our renormalization group, so that

$$\frac{d\mu}{dl} = \zeta \mu . \tag{5.19}$$

This renormalization procedure can be extended to G_3^c and higher-order cluster integrals. Although the coupling constant recursion relations so obtained turn out to be slightly different from (5.15) and from each other, these differences vanish in the limit $L \rightarrow \infty$. Furthermore, these cluster integrals are higher order in v than G_2^c, and should become negligible as $\bar{v}(l)$ iterates to zero.

C. Flory limit and the constitutive relation

For large l, this renormalization group takes us into a region of weak coupling and high vortex densities, where the mean-field theory of Sec. IV C is valid. Instead of proceeding immediately to the matching calculations, we will take a brief detour to rederive the results of Sec. IV C with a mean-field theory for the path integral partition function. Upon defining a δ function with a momentum shell cutoff

$$\delta_\Lambda^{(d)}(\mathbf{x}) = \frac{1}{\Omega} \sum_{k<\Lambda} e^{i\mathbf{k}\cdot\mathbf{x}} , \tag{5.20}$$

we rewrite the Hamiltonian (5.3) as

$$\frac{H}{k_B T} = \tfrac{1}{2} K \int_0^L dz \sum_{i=1}^N \left| \frac{d\mathbf{r}_i}{dz} \right|^2 + \tfrac{1}{2} \sum_{i=1}^N \int_0^L dz \sum_{\substack{j=1 \\ j\neq i}}^N v_0 \delta_\Lambda^{(d)}[\mathbf{r}_i(z) - \mathbf{r}_j(z)] . \tag{5.21}$$

The smeared δ function has a finite spatial extent $\lambda \sim \Lambda^{-1}$. If the vortex lines are packed together tightly, so that the average spacing is much less than λ, we can write

$$\sum_{\substack{j=1 \\ j\neq i}}^N \delta_\Lambda^{(d)}[\mathbf{r}_i(z) - \mathbf{r}_j(z)] \approx n . \tag{5.22}$$

Because the vortex lines are noninteracting in this approximation, the path integral partition function is trivial

$$Z_N = e^{-(1/2) N L n v_0} \frac{Z_1^N}{N!} . \tag{5.23}$$

The physics of this high-density limit is much the same as the Flory limit for a polymer melt.[16]

The free energy of N vortex lines is given by the logarithm of the partition function

$$\frac{A(N)}{k_B T} = -\ln Z_N = \frac{N^2 L v_0}{2\Omega} - N \ln Z_1 + \ln N! . \tag{5.24}$$

Minimizing the Gibbs energy

$$G = A(N) - \mu L N \tag{5.25}$$

with respect to N yields the mean-field constitutive relation

$$\frac{\tilde{\mu}}{k_B T} = n v_0 , \tag{5.26}$$

where the "renormalized" chemical potential $\tilde{\mu}$ is given by (4.28). This is equivalent to (4.26), which was derived from a mean-field theory of the coherent-state functional integral. Using (4.11), we can evaluate $\tilde{\mu}$ in the large L limit

$$\begin{aligned}\tilde{\mu} &\equiv \mu - \frac{k_B T}{L} \ln \frac{N}{Z_1} \\ &= \mu + \frac{k_B T}{b} \ln q .\end{aligned} \tag{5.27}$$

The correction to μ is due to the entropy per unit length of the random-walk fluctuations of a single vortex line. We can define a renormalized critical field H_{c1}^R by $\tilde{\mu} \equiv (H - H_{c1}^R)\phi_0/4\pi$. Then

$$H_{c1}^R = H_{c1} - \frac{4\pi k_B T}{b\phi_0} \ln q = H_{c1} - \frac{4\pi k_B T}{b\phi_0} \ln \left(\frac{2\pi b k_B T}{\tilde{\epsilon}_1 a^2} \right) , \tag{5.28}$$

where we have used Eq. (4.11b). The critical field is renormalized downward because vortex lines become easier to create for $T > 0$.

We begin the matching calculation by substituting renormalized parameters in (5.26),

$$\frac{\tilde{\mu}(l)}{k_B T} = n(l) v(l) , \tag{5.29}$$

and search for a value of l such that this mean-field relation is sensible. We again focus on the infinite L limit for simplicity, and set $\zeta = 2$ so that $K(l)$ remains fixed. For large l, the recursion relation solution (5.17) behaves like $\bar{v}(l) \approx 1/K_2 l$. Upon substituting $K_2 = 1/2\pi$ and using the definition $\bar{v} \equiv vK$, we obtain

$$v(l) \approx \frac{2\pi}{Kl} . \tag{5.30}$$

We also need the other renormalized quantities

$$\tilde{\mu}(l) = e^{2l} \tilde{\mu}_0 , \quad n(l) = e^{2l} n_0 \tag{5.31}$$

to transform (5.26) into

$$\frac{\tilde{\mu}_0}{k_B T} = \frac{2\pi n_0}{Kl} . \tag{5.32}$$

To ensure that the mean-field theory is valid, we iterate until $n(l^*)\lambda^2 \sim 1$ and derive

$$\frac{\tilde{\mu}}{k_B T} = \frac{4\pi n}{K \ln(1/n\lambda^2)} , \tag{5.33}$$

where we have dropped the subscripts on the bare quantities. Upon setting $K = \tilde{\epsilon}_1/k_B T$, and solving for $n = B/\phi_0$, we obtain the result (1.6) quoted in the Introduction[2] with H_{c1}^R substituted for H_{c1}. How thick must the sample be for (5.33) to be valid? If the recursion relation (5.16) is to be a good approximation for (5.15), we must have $\Lambda^2 L(l)/K \gg 1$ at all stages of the iteration. This will be true provided that

$$\frac{\Lambda^2 L_0}{K} \gg e^{2l^*} = \frac{1}{n_0 \lambda^2} , \tag{5.34}$$

or equivalently $L_0 \gg \xi_z$: The sample must be thicker than the entanglement correlation length (3.12), which is the same as (3.13).

The structure factor obeys the homogeneity relation

$$S(\mathbf{q}_\perp, q_z, K, \tilde{\mu}, n) = S(e^l \mathbf{q}_\perp, e^{2l} q_z, K, e^{2l}\tilde{\mu}, e^{2l} n) , \tag{5.35}$$

for $\zeta = 2$. Again iterating the renormalization-group transformation until $n(l^*)\lambda^2 \sim 1$, we can evaluate the right-hand side using the mean-field expression (4.51). Using the homogeneity relation

$$\varepsilon(e^l q_\perp, e^{2l}\tilde{\mu}) = e^{2l} \varepsilon(q_\perp, \tilde{\mu}) \tag{5.36}$$

for the Bogoliubov spectrum, we find that all factors of e^l in (5.35) cancel out. Thus the formula (4.51) can be used without alteration even near H_{c1} provided that n is given by the fluctuation-corrected constitutive relation (1.6).

VI. PINNING AND DYNAMICS OF ENTANGLED FLUX LIQUIDS

Thus far, we have neglected the pinning centers which are responsible for suppression of flux flow resistivity at high fields in conventional superconductors.[15] As discussed in Ref. 2, strong pinning could destroy or modify any of the phases discussed here, including the Abrikosov flux lattice. Among the possibilities are an equilibrium entangled flux liquid in which disorder dominates the effects of thermal fluctuations. The numerical results of Kardar and Zhang for random walks in a random medium[37] show that an isolated flexible vortex line will wander even further than its thermal counterpart in the presence of disorder,[2]

$$\sqrt{\langle |\mathbf{r}(z) - \mathbf{r}(0)|^2 \rangle} \propto |z|^\nu ,$$

with $\nu \approx 0.62 \pm 0.04$, which should be contrasted with Eq. (3.10). As pointed out by Natterman and Lipowsky,[38] Eq. (6.1) leads to a $B(H)$ constitutive relation near H_{c1} of the form

$$B(H) \propto (H - H_{c1})^{\bar{\beta}} ,$$

where $\bar{\beta} = \nu/(1-\nu) \approx 1.5$, instead of the linear dependence with a logarithmic correction shown in Eq. (1.6).

The effects of random impurities on the Abrikosov flux lattice have been discussed by Larkin and Ovchinnikov,[39] who conclude that impurities inevitably break up translational order on scales larger than a disorder-induced correlation length. These arguments predate, but are similar to standard arguments for the destruction of long-range order in the random field XY model below four dimensions.[40] Very short translational and orientational correlation lengths are in fact evident in the low temperature, low-field Bitter photographs of Ref. 5. We would expect, however, larger disorder-induced correlation lengths at higher fields, where the flux lattice is stiffer (the disorder-induced correlation length in Ref. 39 is proportional to $K^{1/2}\mu^{3/2}d^2$), and at higher temperatures, where thermal fluctuations can blur out some of the disor-

der.[41,42] The thermal fluctuations which are so prevalent in high-T_c superconductors have been incorporated into the Larkin-Ovchinnikov theory of flux pinning by Feigel'man and Vinokur.[43] Fisher has argued that the crystalline phase is replaced by a distinct thermodynamic "vortex glass" phase in the presence of disorder.[44]

Disorder will be most effective in suppressing flux flow resistivity in vortex phases which exhibit a nonzero shear modulus on experimental time scales. In conventional superconductors, for example, a few securely pinned flux lines can pin the entire flux lattice if there is a large shear rigidity. We argue here that very long shear relaxation times may also be possible in an entangled flux liquid. Although it will greatly affect the response to a dilute concentration of pinning centers, this mechanism for obtaining a shear modulus does not require pinning centers to work.

Figure 9 shows a heavily entangled flux liquid, viewed down the z axis. Each flux line executes a two-dimensional random walk, occasionally entwining around one of its near neighbors. Figure 9 is like a two-dimensional polymer melt, with the understanding that polymers which appear to cross in the projection are actually ordered, one above the other, according to which of the crossing lines has the largest z coordinate. As in Sec. V, the z coordinate plays the role of a monomer index in this polymer analogy.

If the configuration of vortex lines in Fig. 9 is subject to a shear stress σ_{xy}, the constraints provided by the entanglements in this figure will make relaxation difficult. The notion of constraints requires a large barrier to flux line cutting.[45] When two lines, both approximately parallel to **H**, cross, they must pass over a barrier of order $2\epsilon_1 l$, where ϵ_1 is the line tension, and l is the distance along **H** over which the crossing occurs. Upon expressing ϵ_1 in terms of the lower critical field, we find

$$\frac{2\epsilon_1 l}{k_B T} = \frac{H_{c1}\phi_0 l}{2\pi k_B T} \approx 50 , \tag{6.1}$$

where we have set $H_{c1}=80$ Oe, $l=10$ Å, and $T=77$ K. Thus, line crossings will be very difficult, just as for polymers in an entangled melt.

The analogy with polymer melts[16] suggests that, after an initial transient, the strain u_{xy} will be proportional to the applied stress for times $t < \tau_L$,

$$u_{xy} \approx \sigma_{xy}/\mu_0 , \tag{6.2}$$

which defines a shear modulus μ_0 for times shorter than the relaxation time τ_L. For times longer than τ_L, the material will behave like a viscous liquid, with the strain rising linearly with t,

$$u_{xy} \approx \sigma_{xy} t/\eta , \tag{6.3}$$

which defines a shear viscosity η. The key quantity in this description of the viscoelastic response is the relaxation time τ_L, which, for polymers, is a strong function of the polymerization index.

The analogous time scale in entangled flux liquids will be a sensitive function of the sample thickness L. To estimate this time, we use the de Gennes reptation theory of polymeric relaxation in three dimensions,[16] in which each polymer is assumed to diffuse along a "tube" defined by the entanglement constraints. A very similar situation arises in the two-dimensional polymeric problem considered here. The de Gennes theory predicts that τ_L varies approximately as the cube of the sample thickness

$$\tau_L = \tau_0 (L/\xi_{z'})^3 , \tag{6.4}$$

where τ_0 is a microscopic time, and we expect that $\xi_{z'}$ is of the order of the entanglement correlation length. Motion of the center of mass of a single vortex line is described by the diffusion constant[16]

$$D_L = D_0 (L/\xi_{z'})^{-2} , \tag{6.5}$$

where D_0 is the diffusion constant of a point vortex in, say, an isolated CuO_2 plane. A rough estimate is $D_0 \sim \hbar/m_e \sim 1$ cm^2/sec. The microscopic relaxation time should be of order

$$\tau_0 \sim 1/D_0 n\phi_0 \sim 1/D_0 B . \tag{6.6}$$

If the intervortex spacing is $d=(\phi_0/B)^{1/2} \approx 100$ Å and $\xi_{z'}=2000$ Å, we find from Eq. (6.4) that $\tau_L = 10^3$ sec or about 15 min for $L=1$ cm. The shear viscosity in this regime should be of order[16]

$$\eta \approx \tau_L \mu_0 , \tag{6.7}$$

or $\eta \approx 2\times 10^4$ poise if we estimate μ_0 from (2.18) with $H = \frac{1}{2} H_{c2}$.

The ideas sketched above are far from a complete theory of the dynamics of a heavily entangled flux liquid. They do suggest, however, that regimes of very high viscosity (over 10^6 times that of water) are possible in sufficiently thick samples. One might even speculate on a polymerlike glass transition with decreasing temperature as the origin of the "irreversibility lines" like those discussed by Malozemoff *et al.*[46]

Note added in proof: (a) After this paper was accepted for publication, we learned of work by A. Houghton, R. A. Pelcovits, and A. Sudbø, which revises Ref. 23 to incorporate both an anisotropic tilt modulus and nonlocal elastic constants into the Lindemann criterion. These authors obtain good fits to the melting curves of Ref. 3 with this approach. (b) We would also like to direct readers' attention to the recent paper by G. T. Dolan, G. V. Chandrasekar, T. R. Dinger, C. Feild, and F. Holtzberg, Phys. Rev. Lett. **62**, 827 (1989), which presents low-temperature Bitter decorations of triangular flux lattices

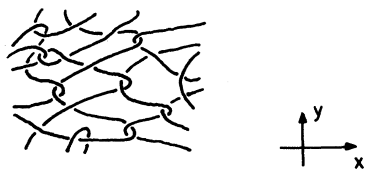

FIG. 9. Schematic top view of an entangled flux liquid. This figure effectively projects the vortex configuration along the z axis, and makes the system resemble an entangled, two-dimensional polymer melt.

in Y-Ba-Cu-O with very large translational correlation lengths even in low fields. (c) D. Huse has pointed out that there are residual electromagnetic contributions to the line tension which invalidate Eq. (3.4) in the limit of very low fields and small M_1/M_3. As a result, $\tilde{\epsilon}_1$ will be larger than suggested by Eq. (3.6) in the low-field limit, and one will have to go closer to T_c to observe the prediction (1.6). We are grateful to Dr. D. Huse for this observation and refer readers to J. W. Ekin, B. Serin, and J. R. Clem, Phys. Rev. B **9**, 912 (1974) for a detailed discussion of the electromagnetic effect in conventional superconductors.

ACKNOWLEDGMENTS

One of us (D.R.N.) has benefited considerably from the advice of R. B. van Dover, R. S. Markiewicz, and, especially, D. J. Bishop on the experimental situation. We are also grateful for stimulating conversations with D. Ceperley, B. I. Halperin, P. C. Martin, and M. Tinkham. This work was supported by the National Science Foundation through Grant No. DMR88-17291 and through the Harvard Materials Research Laboratory. H.S.S. would like to acknowledge support from the U.S. Office of Naval Research.

[1]M. Rice, Z. Phys. B **67**, 141 (1987).
[2]D. R. Nelson, Phys. Rev. Lett. **60**, 1973 (1988).
[3]P. L Gammel, L. F. Schneemeyer, J. V. Waszczak, and D. J. Bishop, Phys. Rev. Lett. **61**, 1666 (1988).
[4]R. B. van Dover, L. F. Schneemeyer, E. M. Gyorgy, and J. V. Waszczak, Phys. Rev. B (to be published).
[5]P. L. Gammel, D. J. Bishop, G. J. Dolan, J. R. Kwo, C. A. Murray, L. F. Schneemeyer, and J. V. Waszczak, Phys. Rev. Lett. **59**, 2592 (1987).
[6]See, e.g., D. R. Nelson, in *Phase Transitions and Critical Phenomena,* edited by C. Domb and J. L. Lebowitz (Academic, New York, 1983), Vol. 7, p. 1.
[7]D. S. Fisher, Phys. Rev. B **22**, 1190 (1980).
[8]M. P. A. Fisher and D. H. Lee, Phys. Rev. B **39**, 2756 (1989).
[9]P. G. de Gennes and J. Matricon, Rev. Mod. Phys. **36**, 45 (1964).
[10]J. W. Negele and J. Orland, *Quantum Many-Particle Systems* (Addison-Wesley, New York, 1988), Chaps. 1 and 2.
[11]V. N. Popov, *Functional Integrals and Collective Excitations* (Cambridge Univ. Press, New York, 1987).
[12]D. Cribier, B. Jacrot, L. M. Rao, and B. Farnoux, Phys. Rev. Lett. **9**, 106 (1964).
[13]See, e.g., S. N. Coppersmith, D. S. Fisher, B. I. Halperin, P. A. Lee, and W. F. Brinkman, Phys. Rev. B **25**, 349 (1982).
[14]A. L. Fetter and P. C. Hohenberg, in *Superconductivity,* edited by R. D. Parks (Dekker, New York, 1969), Vol. 2.
[15]M. Tinkham, *Introduction to Superconductivity* (McGraw-Hill, New York, 1975).
[16]P. G. de Gennes, *Scaling Concepts in Polymer Physics* (Cornell Univ. Press, Ithaca, 1979).
[17]See, for example, V. G. Kogan, Phys. Rev. B **24**, 1572 (1981).
[18]B. Batlogg, T. T. M. Palstra, L. F. Schneemeyer, R. B. van Dover, and R. J. Cava, Physica C **153-155**, 1062 (1988).
[19]L. J. Campbell, M. M. Doria, and V. G. Kogan, Phys. Rev. B **38**, 2439 (1988).
[20]R. Labusch, Phys. Status Solidi **32**, 439 (1969).
[21]A. L. Fetter, P. C. Hohenberg, and P. Pincus, Phys. Rev. **147**, 140 (1966).
[22]Related treatments of the Lindemann criterion using, however, an *isotropic* estimate such as (2.16) for the tilt modulus, have been presented by A. Houghton and R. A. Pelcovits (unpublished); see also, M. V. Feigel'mann and V. M. Vinokur (unpublished).
[23]M. A. Moore, Phys. Rev. B (to be published) uses a Lindemann criterion in a different way to estimate the onset of flux lattice melting. Building on work by D. Maki and H. Takayama [Prog. Theor. Phys. **46**, 1651 (1971)] and G. Eilenberger [Phys. Rev. **164**, 628 (1967)], he proposes a continuum elastic theory which depends only on the shear modulus and the superfluid density. This elastic free energy, however, appears to lead to a divergent energy when the flux lines are tilted, in contrast with the finite tilt elastic constant predicted by Eq. (2.16). Tilt energies are determined by a superfluid density which vanishes as $H \rightarrow H_{c2}$ in Moore's theory, rather than by the macroscopic magnetic response as discussed here. The crossover from Moore's description to the one used here occurs at long wavelengths, and can be understood using the nonlocal elastic constants derived by Brandt; see E. H. Brandt and U. Essman, Phys. Status Solidi **144**, 13 (1987), and references therein.
[24]V. G. Kogan and L. J. Campbell (unpublished).
[25]For a similar problem in the elastic theory of rare-gas atoms adsorbed on graphite, see Appendix C of D. R. Nelson and B. I. Halperin, Phys. Rev. B **19**, 2457 (1979).
[26]R. S. Markiewicz, J. Phys. C **21**, L1173 (1988).
[27]See, e.g., P. C. Hohenberg, A. Aharony, B. I. Halperin, and E. D. Siggia, Phys. Rev. B **13**, 2986 (1979), and references therein. For a related analysis of dimensional crossover in a slab of superfluid helium, see Appendix C of V. A. Ambegaokar, B. I. Halperin, D. R. Nelson, and E. D. Siggia, Phys. Rev. B **21**, 1806 (1980).
[28]S. Ostlund and B. I. Halperin, Phys. Rev. B **23**, 335 (1981).
[29]R. P. Feynman and A. R. Hibbs, *Quantum Mechanics and Path Integrals* (McGraw-Hill, New York, 1965); R. P. Feynman, *Statistical Mechanics* (Benjamin, Reading, 1972).
[30]D. M. Ceperley and E. L. Pollock, Phys. Rev. Lett. **56**, 351 (1986); E. L. Pollock and D. M. Ceperley, Phys. Rev. B **36**, 8343 (1987); and (unpublished).
[31]We note, however, that this issue is not yet settled in the closely related problem of entangled polymer melts, where there may actually be a phase transition as function of the polymerization index N. See T. A. Kavassalis and J. Noolandi, Phys. Rev. Lett. **59**, 2674 (1987).
[32]A. A. Abrikosov, L. P. Gorkov, and I. E. Dzyaloshinski, *Methods of Quantum Field Theory in Statistical Physics* (Prentice-Hall, New York, 1963).
[33]S. F. Edwards, Proc. Phys. Soc. London **85**, 613 (1965); J. des Cloizeaux, J. Phys. (Paris) **43**, 635 (1981).
[34]A very similar situation arises in renormalization-group treatments of d-dimensional bosons at low temperatures; see D. S. Fisher and P. C. Hohenberg, Phys. Rev. B **37**, 4936 (1988).
[35]M. Muthukumar and B. G. Nickel, J. Chem. Phys. **80**, 5839 (1984).
[36]J. E. Mayer and M. G. Mayer, *Statistical Mechanics* (Wiley, New York, 1977). For a related quantum virial expansion, see R. K. Pathria, *Statistical Mechanics* (Pergamon, New

York, 1984), Sec. 9.7.
[37]M. Kardar and Y.-C. Zhang, Phys. Rev. Lett. **58**, 2087 (1987).
[38]T. Natterman and R. Lipowsky, Phys. Rev. Lett. **61** 2508 (1988).
[39]A. I. Larkin, Zh. Eksp. Teor. Fiz. **58**, 1466 (1970) [Sov. Phys. JETP **31**, 784 (1970)]; A. I. Larkin and Yu N. Ovchinnikov, J. Low Temp. Phys. **34**, 409 (1979).
[40]Y. Imry and S. K. Ma, Phys. Rev. Lett. **35**, 1399 (1975).
[41]For an example of a translationally disordered system which becomes crystalline with *increasing* temperature (reentrant melting) for similar reasons, see D. R. Nelson, Phys. Rev. B **27**, 2902 (1983).
[42]Natterman and Lipowsky (Ref. 38) suggest that the random-field model overestimates the effect of pinning, and argue that a three-dimensional flux lattice is in fact *stable* to *weak* pinning.
[43]Feigel'man and Vinokur, Ref. 22.
[44]M. P. A. Fisher, Phys. Rev. Lett. **62**, 1415 (1989); see also S. John and T. C. Lubensky, Phys. Rev. B **34**, 4815 (1986).
[45]E. J. Brandt, J. R. Clem, and D. G. Walmsley, J. Low Temp. Phys. **37**, 43 (1979).
[46]A. P. Malozemoff, T. K. Worthington, Y. Teshurun, and F. Holtzberg, Phys. Rev. B **38**, 7203 (1988), and references therein.